Fischer-Tropsch reaction over alumina-supported cobalt catalyst: activation using H_2 and CO

Master's Dissertation

Report submitted in partial fulfilment of

Magister Technologiae

In

Chemical Engineering

In the

FACULTY OF EGINEERING AND THE BUILT ENVIRONMENT

Of the

University of Johannesburg

Compiled by : Phathutshedzo Rodney Khangale
Student Number : 201011724
Supervised by : Prof Kalala Jalama
Co-Supervised by : Prof Reinout Meijboom

Submitted: 04th January 2016

DECLARATION

I hereby declare that this dissertation which, I hereby submit in fulfilment of the qualification of: M.TECH in CHEMICAL ENGINEERING to the University of Johannesburg, Department of Chemical Engineering is, apart from the recognized assistance from my supervisors, my own work which has not previously been submitted by me or any other person to any institution to obtain a diploma or degree.

_____

Signature of candidate

04th day of January 2016

ABSTRACT

The catalytic activity for Fischer-Tropsch (FT) reaction over cobalt-based catalysts mainly depends on two parameters, namely the reducibility of cobalt precursors and cobalt dispersion. Therefore, a perfect catalyst would comprise of an optimal combination of these two parameters. Cobalt precursor's reduction is usually performed in the presence of H_2 and is usually limited by metal-support interactions which, in some cases, lead to the formation of metal-support compounds that are not reducible under a practical reduction temperature range. The water vapour that is formed during cobalt-based reduction by H_2 has been reported to promote the formation of these metal-support compounds in some cases. An investigation on a reduction process that does not produce water would potentially offer opportunities for better cobalt-based catalyst reduction. Therefore, the aim of this project was to investigate the effect of activating Co/Al_2O_3 FT catalyst using H_2 or CO on the catalyst structure and performance for FT reactions. The catalyst was prepared by impregnation of the support (Al_2O_3) with a cobalt nitrate ($Co(NO_3)_2 \bullet 6H_2O$) solution and calcined in air at 500°C for 10 hours to decompose and transform the cobalt nitrate to cobalt oxide. XRD analysis was performed to determine the structure of the catalyst prepared. BET analysis was performed to determine the surface area and porosity of the catalyst. Temperature programmed reduction (TPR) was performed on calcined Co/Al_2O_3 catalyst using a H_2 and CO containing gas mixture respectively to study the reduction behaviour of the catalyst. The catalyst morphology was studied using scanning electron microscopy (SEM) analysis. The catalyst was tested for FT reaction in a fixed bed reactor and the outlet gas products were analysed using a Dani master gas chromatograph (GC) equipped with thermal conductivity detector (TCD) and flame ionisation detector (FID).

It was found that CO activates the Co/Al_2O_3 catalyst at a lower temperature than H_2 and is accompanied by carbon deposition on the catalyst surface. The main forms of cobalt species in catalyst samples reduced by CO or H_2 at 300 ^oC were CoO. Co^0 and CoO were the major cobalt phases for the catalyst samples respectively reduced by CO and H_2 at 350 ^oC.

The highest catalytic activity for FT reaction with the highest rate of C_{5+} hydrocarbons formation were measured on CO-activated catalyst samples. The deposited carbon on CO-reduced samples is believed to be a precursor for possible cobalt carbide formation during FT reaction that led to high methane selectivity.

ACKNOWLEDGEMENTS

All thanks goes to the following for their input in making this project a success:

My supervisors, Prof Kalala Jalama and Prof Reinout Meijboom for their guidance and passion;

University of Johannesburg, Department of Metallurgy, for assisting with XRD and SEM analyses;

University of Johannesburg, Department of Chemistry meta-catalysis group, for assisting with BET and TPR analyses;

National Research Foundation (Renewable and Sustainable Energy Scholarship) and the University of Johannesburg for financial support.

TABLE OF CONTENTS

LIST OF FIGURES

CHAPTER 3

CHAPTER 4

LIST OF TABLES

CHAPTER 4

LIST OF ABBREVIATIONS AND SYMBOLS

ASF: Anderson-Schulz-Flory

BET: Brunnauer, Emmett and Teller

FID: Flame Ionisation Detector

FT: Fischer-Tröpsch

FTS: Fischer-Tröpsch Synthesis

GC: Gas Chromatograph

Syngas/SG: Synthesis gas ($CO + H_2$)

TCD: Thermal Conductivity Detector

TOF: Turnover frequency (s^{-1})

TPR: Temperature Programmed Reduction

WGS: Water-Gas-Shift

XRD: X-ray Diffraction

α: Chain growth probability

CHAPTER 1: INTRODUCTION

1.1. Background

Fischer-Tropsch (FT) synthesis is a group of chemical reactions that transforms the combination of CO and H_2 into liquid hydrocarbons [1]. It was initially established in 1925, by Franz Fischer and Hans Tropsch. The process has been considered as another way of producing a transportation fuel, from typically coal, biomass or natural gas with low emission of pollutants. The FT process is considered as the origin of low-sulphur diesel fuel and increases the supply of petroleum-derived hydrocarbons.

A good cobalt-support interaction is one of essential properties to achieve a high quality catalytic performance as it is intensely associated with Co_3O_4 reducibility [2]. Cobalt catalyst surface properties are influenced by the cobalt particles nature and the preparation techniques, which may result in the strong interaction between cobalt and the support. Two contradictory parameters play a crucial role when it comes to the catalytic activity for FT reaction: i) metal dispersion and ii) catalyst reducibility. A perfect catalyst would comprise an ideal amalgamation of these two parameters. A Strong interaction between the catalyst and the support is generated by a highly dispersed catalyst and has a tendency to inhibit the catalyst reduction to the metallic state. The type of cobalt precursor used in the preparation of the catalyst may have an impact on the catalyst reducibility and dispersion [3].

The FT process consists of numerous chemical reactions which produce diverse hydrocarbons which are given by the general formula C_nH_{2n+2}. The utmost valuable reactions produce alkanes as follows:

$$(2n+1)H_2 + nCO \rightarrow C_nH_{2n+2} + nH_2O \quad \text{..... (1.1)}$$

Where n is a positive number. The generation of methane (n=1) is not desirable, as methane is a gas at standard temperature and pressure (STP). Most alkanes formed are straight chains. In addition to alkanes formation, competing reactions produce trivial amount of alkenes as well as alcohols and additional oxygenated hydrocarbons.

A range of catalysts may be employed to execute FT synthesis; however the utmost frequently used are the transition metals iron, ruthenium and cobalt. Nickel may as well be ideal on the other hand tends to promote the formation of methane. Cobalt-based catalysts are

very active particularly when the feedstock used is natural gas; however Fe-based catalysts are more appropriate for poor hydrogen syngas derived from low quality feedstocks like coal or biomass [4]. Catalysts are supported with materials with high surface area such as SiO_2, Al_2O_3 or zeolite. Due to good mechanical properties allied with Al_2O_3 as a catalyst support, Al_2O_3-supported catalysts are frequently employed for the FT reaction. Yet, the main problem with the Co/Al_2O_3 catalyst is the imperfect reducibility of Co as the consequence of the strong interaction between the metal and the support [5-9]. Water vapour favours the formation of Co-support composites as it increases the interaction between cobalt metal and the support and by assisting the movement of cobalt ions into the tetrahedral sites of Al_2O_3 to produce non-reducible cobalt aluminate [10-12]. SiO_2 possesses a weaker interaction with Co which results in a low metal (Co^0) dispersion on SiO_2 and a good reducibility of Co_3O_4. FT catalysts are very reactive to poisoning by sulphur. The reactivity of FT catalyst to sulphur is superior for Co based catalysts relative to their iron equivalents [13].

1.2. Problem statement

It is vital for the petrochemical and energy sector to produce transportation products like petrochemicals and high quality fuels with low emission of pollutants. FT is a chemical process which is used to produce petrochemicals and high quality fuels. During FTS; addition of a catalyst is always required. There are various catalysts which can be used in the FTS process. Cobalt catalysts supported either on alumina, titanium dioxide; etc. are used in order to acquire high catalytic activity and favour the formation of longer chain hydrocarbons.

Co-based FT catalysts are prepared using various techniques and calcination is typically the final preparation step which converts cobalt nitrate to cobalt oxide. The active site for FTS is metallic cobalt and thus it is always required to reduce the catalyst before FT synthesis. Generally, Co based catalysts are activated using H_2 [14]. It has been reported in the literature that during reduction with H_2 cobalt oxide species which strongly interact with the support are formed [15]. These compounds limit the reducibility of cobalt oxide to the metallic form and are generally inactive for FTS. Likewise, during reduction with H_2, water is also formed and it has been reported in the open literature that water stimulates the formation of these compounds [10-12]. Metal carbides [16–17] and metal nitrides [16] may possibly also catalyse the FT reaction. Various researchers have discovered some positive effects on the reduction of Co-based catalyst using CO [18]. During cobalt oxide reduction with CO, carbon dioxide is formed instead of water. The question is: can the use of other reducing agents such

as CO which does not form water during cobalt oxide reduction avoid the formation of Co-support compounds and improve the reduction process? According to Karaca et al [19] the presence of CO during reduction prevents a catalyst from forming a strong interaction with the support. This was also suggested by Jongsomjit and Goodwin Jr. who reported that adding CO during H_2 reduction of a Co/Al_2O_3 catalyst caused an increase in catalyst activity relative to the catalyst reduced without CO [20]. Moreover, higher catalytic activity is linked with improved catalytic reducibility.

1.3. Aim and objectives

The aim of this project was to investigate the effect of activating Co/Al_2O_3 Fischer-Tropsch catalyst using H_2 or CO on a catalyst support structure and to establish whether this enhances FT reaction. The specific objectives include:

- Co/Al_2O_3 catalyst synthesis;
- Catalyst reduction using H_2 or CO;
- Catalyst characterization in order to determine the effect of a reducing gas (H_2 or CO) on the catalyst structure and morphology;
- Catalyst testing for FTS in order to evaluate the effect of reducing agents (H_2 or CO) on CO conversion, product distribution and catalyst stability.

REFERENCES

[1]. K. Jalama, J. Kabuba, H. Xiong, L.L. Jewell, Catalysis Communications 17 (2012) 154–159

[2]. I.H. Jang, S.H. Um, B. Lim, M.H. Woo, K-W. Jun, J-B. Lee, J.W. Bae, Applied Catalysis A: General 450 (2013) 88– 95

[3]. K. Jalama, N.J. Coville, D. Hildebrandt, D. Glasser, L.L. Jewell, Applied Catalysis A: General 326 (2007) 164–172

[4]. L. Braconnier, E. Landrivon, I. Clemencon, C. Legens, F. Diehl, Y. Schuurman, Catalysis Today 215 (2013) 18-23

[5]. K. Jalama, N.J. Coville, H. Xiong, D. Hildebrandt, D. Glasser, S. Taylor, A. Carley, J.A. Anderson, G.J. Hutchings, Applied Catalysis A: General 395 (2011) 1–9

[6]. S-J. Park, J.W. Bae, G-I. Jung, K-S. Ha, K-W. Jun, Y-J. Lee, H-G. Park, Applied Catalysis A: General 413– 414 (2012) 310– 321

[7]. L. Shi, Y. Jin, C. Xing, C. Zeng, T. Kawabata, K. Imai, K. Matsuda, Y. Tan, N. Tsubaki, Applied Catalysis A: General 435– 436 (2012) 217– 224

[8]. A.M. Venezia, V.L. Parola, L.F. Liotta, G. Pantaleo, M. Lualdi, M. Boutonnet, S. Järås, Catalysis Today 197 (2012) 18– 23

[9]. U. Cornaro, S. Rossini, T. Montanari, E. Finocchio, G. Busca, Catalysis Today 197 (2012) 101– 108

[10]. A. Kogelbauer, J.G. Goodwin, R.J. Oukaci, Journal of Catalysis 160 (1996) 125

[11]. J.L. Li, X.D. Zhan, Y.Q. Zhang, G. Jacobs, T. Das, B.H. Davis, Applied Catalysis A: General 288 (2002) 203

[12]. A.M. Hilmen, D. Schanke, K.F. Hanssen, A. Holmen, Applied Catalysis A: General 186 (1999) 169

[13]. J.G. Speight, "Hydrocarbons from synthesis gas", 2011

[14]. A. Steynberg, M. Dry, Studies in surface science and catalysis 152 (2004) 533

[15]. G. Jacobs, T.K. Das, Y.Q. Zhang, J.L. Li, G. Racoillet, B.H. Davis, Applied Catalysis A: General 233 (2002) 263

[16]. G.S. Ranhotra, A.T. Bell, J.A. Reimer, Journal of catalysis 108 (1987) 40

[17]. P.M. Paterson, T.K. Das, B.H. Davis, Applied Catalysis A: General 251 (2003) 449

[18]. Z. Pan, D.B. Bukur, Applied Catalysis A: General 404 (2011) 74– 80

[19]. H. Karaca, O.V. Safonova, S. Chambrey, P. Fongarland, P. Roussel, A. Griboval-Constant, M. Lacroix, A.Y. Khodakov, Journal of Catalysis 277 (2011) 14–26

[20]. B. Jongsomjit, J.G. Goodwin Jr., Catalysis Today 77 (2002) 191–204

CHAPTER 2: LITERATURE REVIEW

2.1. Background

As a results of the depletion of petroleum reserves, and crude oil price escalation from the 1980's [1]; it is crucial to move energy resources from petroleum oil to alternative fuels that are more economical and have a reduced negative effect on the environment [2].

Fischer-Tropsch synthesis (FTS) is of substantial importance due to use as a replacement for the fabrication of fresh transport petroleum and chemicals from different sources of carbon such as natural gas, biomass and coal [3]. The full FTS process comprises coal/biomass gasification or natural gas reforming to produce synthesis gas and the catalytic conversions of the latter into liquid hydrocarbons through the following general chemical reaction:

$$(2n + 1)H_2 + nCO \rightarrow C_nH_{2n+2} + nH_2O \quad (2.1)$$

A range of products such as paraffins, alcohols, olefins, and aldehydes are formed during an FT reaction. The required products are those which contain low methane, low alcohol, a high ratio of olefins/paraffins, and a high C_{5+} content. The product state may be manipulated by the reactor type and/or the reaction conditions and by modifying the catalyst [4]. The products generated during the FT process do not contain nitrogen, sulphur or aromatics; this decreases the negative environmental impact of FTS and makes it potential to synthesize high quality liquid fuels [2]. When the synthesis gas is biomass-derived, the process yields a renewable fuel and is carbon neutral.

One of the ultimate challenges in the FTS is to reduce the formation rate of low molecular weight hydrocarbons, predominantly methane, and also increase the formation rate of longer-chain hydrocarbons (C_{5+} selectivity). This is a significant objective on developing new FTS catalysts [5]. For the process to be effective a catalyst's performance plays a critical role in industrial applications.

2.2. Fischer-Tropsch product distribution

The FTS products are generally linear paraffin, whose distribution complies with the Anderson–Schulz–Flory (ASF) model [6].

One form of the ASF model is given below [7]:

$W_n = (\ln^2 \alpha) n\alpha^n$ ……..……..(2.2)

where Wn represents the mass fraction of the products with n = number of carbon atoms and α is the chain growth probability or growth factor.

This kinetic expression can be expressed in logarithmic form as displayed below:

$\log C_n = \log(\ln^2 \alpha) + n\log\alpha$ ……..(2.3)

where Cn = Wn/n = mole fraction (more accurately, the selectivity of carbon fraction to abolish the mass dissimilarities among olefins and the ancillary product paraffin's).

The equation implies that if logCn is plotted against n, a straight line should be obtained (ASF plot) [7].

It is worth mentioning that some deviations from the ASF model have been reported in literature. Most ASF plots present a straight line in the C_4–C_{12} product range [7]. The deviations from the ASF plot could potentially be due to the complications in accomplishing reproducibility and the exact quantifiable analyses of the products varying from gases to waxes [8]. For instance, heavyweight products might not be volatilized at the temperature of the injection port. Condensation in the heated sample lines in programmed systems may well give non-representative sampling. Reaction conditions typical for FT, e.g. testing a new catalyst, can lead to unforeseen and anonymous reactions other than CO hydrogenation, instigating deceptive deviations from the ASF distribution [7].

On the other hand, ASF models with two α values have also been reported. For example Huff Jr. and Satterfield [9] have reported that deprived of alkali promoters, Fe provided a perfect ASF distribution with little value of growth probability (α value of 0.65). When a K-promoted Fe catalyst was used, the product distribution gave a curved ASF plot. These researchers claimed that alkalization of the catalyst produced binary catalytic sites with

differing chain growth features. The un-promoted sites created products with a small α-value; the alkalized sites provided a high α-value. Grounded on this idea, they proposed a mathematical model (known as the two superimposed ASF distribution) and found that 61% of the product was generated on un-alkalized sites with α equal to 0.57 and 39% on alkalized sites with an α value of 0.87.

A greater chain growth probability means that the product comprises mostly of longer chain hydrocarbons, and therefore a reduced amount of CH_4. The selectivity of a catalyst to longer chain hydrocarbons is frequently expressed as the selectivity to C_{5+}. It is known that the higher the pressure, or the lower the temperature and inlet H_2/CO ratio, the greater the value of α. The chain growth probability is also reliant on the characteristics of the catalyst. It is ordinarily recognized that the maximum yield to diesel is reached by first creating wax, which is then hydrocracked into the diesel fraction [10]. In this way the formation of smaller chain hydrocarbon by-products is diminished, particularly CH_4. Today, global Fischer-Tropsch research is motivated on exactly how to prepare catalysts that provide a high α value. An α of about 0.9 is associated with a wax-producing Fischer-Tropsch process, which approximately corresponds to a C-atom selectivity between C_{5+} and C_{10+} (78 % and 74 %, respectively) [11].

2.3. Catalysts used in Fischer-Tropsch synthesis

The FT reaction proceeds in the presence of a catalyst and there are different types of catalysts which can be employed to facilitate the process. Transition metals such as cobalt (Co), iron (Fe) and ruthenium (Ru) are the most commonly used [12]. Nickel (Ni) may, under certain circumstances, also be employed but it tends to favour the formation of methane [13]. For many years the topic of cobalt catalysts for use in the FT reaction, supported with different materials, has been of interest [14]. In general, cobalt catalysts are highly active relative to iron catalysts since a lower reaction temperature is required for it to be active in FTS [15]. It is widely known that Co catalyst activity for FTS is a function of the number of metallic cobalt atoms on the surface [16]. To achieve high dispersion, a variety of catalyst supports are utilised in this reaction, including SiO_2, Al_2O_3, TiO_2 and carbon [17]. Cobalt-based catalysts are generally preferred for the FT reaction particularly when natural gas is used as the feedstock. Iron-based catalysts are recommended for low quality feedstocks such as coal [13].

2.3.1. Iron-based catalysts

Iron-based catalysts are recommended for industrial applications as they display higher activity to the water-gas-shift (WGS) reaction which is essential in the transformation of syngas with inferior H_2/CO ratios (resulting from coal or biomass) and low selectivity toward the formation of CH_4 [18]. Fe catalysts can be employed under a comprehensive range of temperatures (up to 340 °C) and convert syngas at low cost. Furthermore, linear hydrocarbons and oxygenates can be produced under diverse operating conditions over iron catalysts. Nevertheless, the main challenges related with the use of a Fe catalyst takes account of low productivity at high conversion, high olefins selectivity, high water-gas-shift activity, and its poor resistant to swift deactivation from coking, carbon deposition and iron carbide formation [17].

2.3.2. Ruthenium-based catalysts

It is commonly acknowledged that Ru catalysts are the most active catalysts for the FT synthesis. At low temperature and high FT system pressure, it yields longer chain hydrocarbons. The use of Ru metal is limited from concerns of cost and restricted availability. Thus, catalyst improvement is necessary to attain high and stable activity [19]. Tang *et al*. [20] indicated that Ru catalysts have been extensively used to study the FTS reaction mechanism as a result of their higher intrinsic activity which permits one to execute FTS at low temperatures and to acquire higher selectivity towards longer-chain (C_{5+}) hydrocarbons. Supports materials such as SiO_2 [21], Al_2O_3, TiO_2 [22], mesoporous molecular sieves [23] and carbon materials [24] are used in preparing FT catalysts. It is clear from the open literature that the nature of the support displays substantial impact on the morphology, redox property, activity of the catalyst and product selectivity of the subsequent catalysts.

Titania has received a lot of consideration as a support material for metal catalysts as it shows a strong interaction between metal and the support. The carrier impact is commonly known as a strong metal-support interaction (SMSI). According to Vannice and Garten [25], Ru catalysts supported on TiO_2 do not demonstrate advanced catalytic activity but lead to lower methane selectivity and tend to favour the formation of olefins. The activity of a Ru catalyst is influenced by the crystallite structure of the supports. Reducing a rutile-supported catalyst at high temperature resulted in a catalyst with better activity relative to an alumina supported catalysts.

2.3.3. Cobalt-based catalysts

Cobalt based catalysts have been reported to be the most efficient catalysts for FT as a result of their high selectivity to linear hydrocarbon, high activity, and low activity to the water-gas-shift reaction [26]. They are also exceptional when there is a necessity for high chain growth and minimal branching probabilities [27]. Co-based catalysts are generally highly active relative to catalysts based on iron and they proceed under a lower reaction temperature [28]. On the other hand, Co is highly expensive as compared to Fe. For this reason, in order to use Co catalyst in the FT process, an optimum design of the catalyst is vital. This objective can be proficient by means of reducing the Co particle size with the intention of increasing the exposed surface area per unit mass of Co metal. The influence of particle size has been investigated by a number of researchers. The particle size of Co has been associated with the metal-support interactions [29].

It is mostly recognized that the activity of Co catalysts for FT depends on the number of Co sites available. Consequently, supports with high surface area have been used to deposit cobalt with the aim of increasing dispersion of active Co metal species [30]. It is widely reported in the open literature that cobalt catalyst performance during FT is predominantly administered by the reducibility of cobalt oxide to the metallic form and dispersion, both of which are allied with the nature of the support utilized [31].

Recently; various Al_2O_3 supports were studied to define the influence of crystal phase and pore size on the Co catalyst properties and activity [32]. Different Al_2O_3 supports were prepared through calcination at various conditions. It was established that the Co particle structure (e.g. the degree of Co reduction, particle size distribution and dispersion) and Co/Al_2O_3 catalyst activity for FT is primarily influenced by the pore diameter of Al_2O_3 support rather than the crystal phase. The highest catalytic activity was attained using a catalyst supported on Al_2O_3 with adequate surface area (ca. 80 m^2g^{-1}). In addition to Al_2O_3 supports with moderate surface area, the appropriate average pore size of the Al_2O_3 support would improve the Co dispersion and stimulate the formation of Co particle with comparatively identical size, bringing about the increase in Co surface area, turn-over-frequency (TOF) and overall activity. Co is normally deposited on supports with high surface area like SiO_2, Al_2O_3, TiO_2 and carbon materials with the aim to advance the dispersion of active Co metal species [32].

2.4. Activation of cobalt based catalysts

It is always very important to activate a catalyst before an FT reaction [33]. The last step in cobalt-based catalyst preparation usually involves calcination in air that yields cobalt oxides. These species must be reduced to metallic cobalt, the active form for the FT reaction. The reducibility of cobalt plays a central part in the activity of supported cobalt catalysts and on the product selectivity. Cobalt reducibility is determined by cobalt dispersion [34]. High metal dispersion and good reducibility of the catalyst are necessary to achieve higher catalyst activity [15]. These requirements seem conflicting; a strong interaction between cobalt and widely used support materials such as titania, silica, zirconia and alumina produces cobalt species with a high dispersion, but these vastly dispersed cobalt species possibly will be reduced at high temperatures. One way to improve the reducibility of cobalt catalysts is to reduce the interaction between the metal and the support by adding another metal which acts as a catalyst promoter [12]. For instance, adding a second metal on a support prior to addition of cobalt could minimise the interaction between Co and the support material by generating a support enclosed within the second metal [15]. Another way could be an optimal selection of the reducing gas mixture. Therefore, this section will discuss the effect of promoters and the composition of reducing gas mixtures on cobalt catalyst reducibility.

2.4.1. Effect of catalyst promoters

A number of researchers have revealed that adding a small amount of noble metal such as Ru, Re or Pt boosts the activity of cobalt based FT catalysts. However, it is still unclear whether or not these promoters affect the product selectivity [1]. The activity of a supported Co catalyst is a function of the reducibility of Co. To improve Co reducibility, which is well dispersed on a support, a trivial quantity of noble metal such as Pt, Ru, Ir, Re or Pd may be added.

2.4.1.1. Promotion with Ru

There are many researchers who described Ru as a catalyst promoter for cobalt catalysts in the FTS process to improve cobalt reducibility and CO conversion. Ru has been described to enhance the reducibility and activity of supported cobalt catalysts [35, 36]. This has been reported to be the result of hydrogen spillover from Ru being able to advance the reduction of cobalt oxides. Adding Ru has been widely reported to considerably increase the turnover rates on cobalt-based catalysts, and it has been suggested that Ru inhibits the deactivation of

cobalt catalysts by catalysing the hydrogenolysis of carbonaceous deposits [37]. Ru has been reported in the literature [38] to act as a structural promoter for Co-based catalysts which avoids the accumulation of cobalt oxide particles during calcination and results in high activity for FT and improves selectivity for longer chain hydrocarbons.

The existence of Ru in a catalyst moves both Co reduction peaks to lower temperatures [39]. Ru is reported to have an incredible promoting influence on the performance of a cobalt catalyst. Hosseini *et al*. [35] studied the effect of Ru loading on the activity and selectivity of a catalyst using typical FT operating conditions. The outcomes indicated that, up to 1.5% loading, the Ru promoter boosted catalyst activity and longer chain hydrocarbon selectivity. Comparable results over Ru-promoted Co catalysts were found by Xu *et al*. [40]. Based on Kapoor *et al*. [41] findings Ru promoted cobalt-based catalyst tend to favour the formation of C_{5+} hydrocarbons.

2.4.1.2. Promotion with Re

Adding Re to a Co/Al_2O_3 catalyst considerably increased the catalytic activity for FT, while the selectivity stayed unaffected [42]. It was proposed that the higher activity was a result of better reducibility and an increased number of active cobalt sites. Promotion with Re is reported to improve the hydrogenation rate of the CO. Bertole *et al*. [43] studied the effect of Re on the performance of Co catalyst and found that Re did not have an impact on either the catalyst activity or the selectivity of CH_4. The existence of the Re promoter only diminished the CH_4 formation and hardly increased the selectivity of heavy weight hydrocarbons. On the other hand, a Re promoter was noticed to have a small influence on the total gaseous (C_2–C_4) olefin and paraffin distribution.

2.4.1.3. Promotion with Pt

Pt can also act as a catalyst promoter for cobalt-based catalysts. According to Schanke *et al*. [44] adding a small quantity of Pt (0.4 wt.%) can significantly increase the reducibility of supported cobalt-based catalysts. This statement was also supported by Li *et al*. [45] and Jacobs *et al*. [46]. The addition of Pt was found to increase oxygenate formation. Pt as a promoter was found to slightly increase WGS activity and oxygenates production [47]. In addition, the presence of a Pt promoter has been reported to increase CH_4 formation and slightly decrease C_{5+} selectivity. According to Vada et al. [42] promotion with Pt does not

influence the selectivity of hydrocarbon under typical FTS conditions. The apparent turnover frequency (TOF) increase as a result of promotion has been attributed to a higher coverage of sensitive intermediates, and this statement is in agreement with what has been reported by Iglesia [48].

2.4.1.4. Promotion with Pd

Pd has also been known to assist the reduction of cobalt oxides [49, 50]. It is generally known that noble metal promoters advance the extent of Co catalyst reduction and consequently increase the conversion of CO. Pd as a promoter on a cobalt catalyst can act as an adsorption site for H_2 and improve the hydrogenation rate in FTS but has not been noticeably investigated [1]. Such enhancement may possibly provide vital paraffin products and avoid the formation of hard waxes, which are inactive carbons that cause catalyst deactivation. Some researchers revealed that the addition of Pd to Co/SiO_2 caused an increase in the relative fraction of paraffin's during FTS. This influence was credited to a higher concentration of surface hydrogen on the Pd promoter. Osakoo *et al*. [51] related physicochemical properties of Co/SiO_2 prepared by both incipient wetness impregnation in absolute ethanol and precipitation with a reverse micelle technique and their influence on the addition of Pd. They found that adding 0.2%wt of Pd improved the reducibility of cobalt, catalyst activity for FTS and selectivity of paraffins. Moreover, adding 1.0%wt of Pd was found to promote the formation of methane, hence the conversion declined.

2.4.1.5. Promotion with Au

Adding small amount of Au is well-known for improving the reducibility of cobalt oxides [52–54]. According to Jacobs *et al*. [50], adding small amount of Au into Co/Al_2O_3 enhanced cobalt oxide reducibility as well as improved the density of surface cobalt sites. The mechanisms for these promoting effects take account of hydrogen spillover and formation of bimetallic particles. If Au is used as a promoter, the turnover frequencies (TOF) usually decline to a certain value and then become constant, as the amount of metal increases in the catalyst. It is generally acknowledged that Group 11 metals (including Au) segregate to the catalyst surface and mount up first in highly active low coordinated surface sites and as a result this causes the reduction in the TOF [55].

2.4.2. Effect of reducing gas

Traditionally, hydrogen is used for activating cobalt catalysts. However, other reducing mixtures have been considered in order to overcome a number of challenges related to the activation process with hydrogen. Studies involving carbon monoxide and carbon monoxide-containing mixtures used for cobalt catalyst activation are reviewed in this section.

2.4.2.1. Cobalt activation with CO

Generally, reduction of supported a Co catalysts with CO containing gas mixture occurs in a two-step reduction but it is more complex because of cobalt carbide formation and carbon deposition [56]:

Step 1 : $Co_3O_4 + CO \rightarrow CoO + CO_2$ …….. (2.2)

Step 2 : $CoO + CO \rightarrow Co + CO_2$ ……..(2.3)

: $2CoO + CO \rightarrow C + CO_2$ ……..(2.4)

CO has been reported to prevent a catalyst from strong interaction with the support and to lead to rapid cobalt carbide formation [57]. Luo et al. have reported that a catalyst activated using CO outperformed a catalyst activated in the presence of H_2 [58].

Jongsomjit and Goodwin Jr [26] measured a lower methane selectivity when a cobalt-based catalyst was reduced in the presence of CO. Pan and Bukur [59] activated a Co/ZnO Fischer-Tropsch catalyst with CO (25 bar and 215^{o}C) and found that CoO and Co_3O_4 were the main cobalt phases in the catalyst with Co_2C and Co^0 as minor phases. They found that cobalt reduction started to take place at a lower temperature when CO was used as a reducing agent as compared to when H_2 was used. Moreover, the catalyst activated in the presence of H_2 yielded higher CO conversion, lower methane selectivity and higher C_{5+} product selectivity as compared to the catalyst activated using CO. Azizi *et al*. [27] suggested that a catalyst reduced by H_2 showed the best catalytic performance as compared to catalysts reduced using either CO or syngas and had higher selectivity towards C_2-C_4 hydrocarbons and low methane selectivity.

2.4.2.2. Cobalt activation with CO/H_2 mixture

A Co Catalyst activated by syngas for FT was reported to result in higher activity, low selectivity to CH_4, higher selectivity towards C_{5+} hydrocarbon products and higher C_3-C_5 olefin to paraffin ratio as compared to catalyst activated by H_2 during an entire reaction [33]. This was explained by better catalyst reduction and dispersion for syngas-reduced catalyst samples. Catalyst activation by syngas was reported to be followed by the formation of carbon nanostructures, which are catalysed by cobalt particles [60]. The reduction of the cobalt oxide to metallic cobalt perhaps may be preferred to the use of H_2 in syngas, and the sintering of cobalt catalyst particles could be prevented by the formation of carbon nanostructures supporting the dispersion of cobalt particles. Pan *et al.* [61] reported the lowest quantity of methane over a cobalt catalyst activated in CO/SG.

2.4.2.3. Sequential activation with $H_2/CO/H_2$

Activation of a cobalt catalyst by reduction in the presence of H_2 followed by carburization in CO followed by reduction with H_2 treatment ($H_2/CO/H_2$) gave good catalytic activity (i.e. resulted in higher conversion of carbon monoxide and higher rate of reaction per unit mass of a catalyst), and did not influence product selectivity, and increased activity and improved selectivity [61]. The composition of a reducing gas mixture and the temperature at which the catalyst is activated has an impact on the different phases of cobalt which can be formed which can in turn have an effect on the performance of the catalyst [60]. Thus, not only metallic cobalt metal (Co^0) will be available after activation, but different phases of cobalt carbides and oxides can be obtained when H_2, CO or a H_2 + CO mixture (syngas) are used. It has been testified in the literature that a three-step activation process involving H_2 reduction, followed by carburization in CO and later H_2 treatment ($H_2/CO/H_2$ activation) resulted in enhanced activity with no influence on selectivity [57] and gave both superior activity and better selectivity [62]. The existence of a hexagonal metallic cobalt phase which is produced in the last stage of reduction (activation) is related to the high catalytic activity. The BET surface area and the pore volume was reduced when the catalyst was activated with CO/SG relative to a CO activated catalyst hence the size of the pore did not considerably change [61].

Pan et al [61] established that activation of the catalyst, expressed in terms of CO conversion, tended to follow the following sequence: CO reduced < H_2 reduced < CO/SG reduced. In

addition, the catalyst activated in the presence of CO/SG was described to give the best activity and generated the lowest quantity of methane which is an undesirable component in FT reaction. Differences in methane selectivity are ascribed to dissimilarities in the degree of conversion; therefore poor methane selectivity is allied with advanced conversion. Cobalt based catalyst performance in the FT reaction depends on the availability and the quantity of active sites of cobalt [63].

REFERENCES

[1]. M.E. Dry, Catalysis Today 71 (2002) 227–241

[2]. K. Asami, A. Iwasa, N. Igarashi, S. Takemiya, K. Yamamoto, K. Fujimoto, Catalysis Today 215 (2013) 80–85

[3]. T. Li, Y. Yang, Z. Tao, C. Zhang, H. Xiang, Y. Li, Fuel Processing Technology 90 (2009) 1247–1251

[4]. M. Arsalanfar, A.A. Mirzaei, H.R. Bozorgzadeh, Journal of Industrial and Engineering Chemistry 19 (2013) 478–487

[5]. S. Karimi, A. Tavasoli, Y. Mortazavi, A. Karimi, Applied Catalysis A: General 499 (2015) 188–196

[6]. C. Xing, J. Suna, G. Yang, W. Shen, L. Tana, P. Zhu, Q. Wei, J. Li, M. Kyodo, R. Yang, Y. Yoneyama, N. Tsubaki, Fuel Processing Technology 136 (2015) 68–72

[7]. I. Puskas, R.S. Hurlbut, Catalysis Today 84 (2003) 99–109

[8]. M. Inoue, T. Miyake, T, Inui, 105 (1987) 266-269

[9]. G.A. Huff, JR., C. Satterfield, Journal of catalysis 85 (1984) 370-379

[10]. T. T. Phadi, MSc. Thesis, University of the Witwatersrand, 2008

[11]. S. L Soled, E. Iglesia, R. A Fiato, J.E. Baumgartner, H. Vroman and S. Miseo, Topics in Catalysis.2003, 26, 101

[12]. N.N. Madikizela-Mngangeni, N.J. Coville, Applied Catalysis A: General 272 (2004) 339–346.

[13]. I.H. Jang, S.H. Um, B. Lin, M.H. Woo, K. Jun, J. Lee, J.W. Bae, Applied Catalysis A: General 450 (2013) 88–95.

[14]. N. Fischer, E. van Steen, M. Claeys, Journal of Catalysis 299 (2013) 67–80.

[15]. J. Hong, W. Chu, P.A. Chernavskii, A.Y. Khodakov, Applied Catalysis A: General 382 (2010) 28–35.

[16]. M. Moyoa, M.A.M. Motchelahoa, H. Xiong, L.L. Jewell, N.J. Coville, Applied Catalysis A: General 413– 414 (2012) 223– 229

[17]. T. Fu, Y. Jiang, J. Lv, Z. Li, Fuel Processing Technology 110 (2013) 141–149.

[18]. T. Fu, Z. Li, Chemical Engineering Science 135 (2015) 3 - 20

[19]. T. Herranz, S. Rojas, F.J. Perez-Alonso, M. Ojeda, P. Terreros, J.L.G. Fierro, Applied Catalysis A: General 311 (2006) 66–75

[20]. H-q. Tang, J-l Li, Journal of fuel chemistry and technology 39(8) (2011) 615–620

[21]. H.Y. Gao, H.W. Xiang, Y.W. Li, Chinese Journal of Catalysis 31(3) (2010) 307–312

[22]. H. Karaca, O.V. Safonova, S. Chambrey, P. Fongarland, P. Roussel, A. Griboval–Constant, M. Lacroix, A.Y. Khodakov, Journal of Catalysis 277 (2011) 14–26

[23]. J. Li, G. Jacobs, Y. Zhang, T. Das, B.H. Davis, Applied Catalysis A: General 223 (2002) 195–203

[24]. M.K. Gnanamani, G. Jacobs, U.M. Graham, W. Ma, V.R.R. Pendyala, M. Ribeiro, B.H. Davis, Catalysis Letters 134 (2010) 37–44

[25]. M.A. Vannice, R.L. Garten, Journal of catalysis 63 (1980) 255–260

[26]. B. Jongsomjit, J.G. Goodwin Jr., Catalysis Today 77 (2002) 191–204

[27]. H.R. Azizi, A.A. Mirzaei, M. Kaykhaii, M. Mansouri, Journal of Natural Gas Science and Engineering 18 (2014) 484–491

[28]. M.J. Parniana, A.T. Najafabadi, Y. Mortazavi, A.A. Khodadadi, I. Nazzari, Applied Surface Science 313 (2014) 183–195

[29]. V.R.R. Pendyala, G. Jacobs, W. Ma, J.L.S. Klettlinger, C.H. Yen, B.H. Davis, Chemical Engineering Journal 249 (2014) 279–284

[30]. K. Shimura, T. Miyazawa, T. Hanaoka, S. Hirata, Applied Catalysis A: General 460–461 (2013) 8–14

[31]. H. Wu, Y. Yanga, H. Suo, M. Qing, L. Yan, B. Wu, J. Xu, H. Xiang, Y. Li, Journal of Molecular Catalysis A: Chemical 390 (2014) 52–62

[32]. K. Shimura, T. Miyazawa, T. Hanaoka, S. Hirata, Journal of Molecular Catalysis A: Chemical 394 (2014) 22–32

[33]. K. Jalama, J. Kabuba, H. Xiong, L.L. Jewell, Catalysis Communications 17 (2012) 154–159

[34]. N. Osakoo, R. Henkel, S. Loiha, F. Roessner, J. Wittayakun, Applied Catalysis A: General 464-465 (2013) 269–280.

[35]. S.A. Hosseini, A. Taeb, F. Feyzi, F. Yaripour, Catalysis Communications 5 (2004) 137–143.

[36]. A. Kogelbauer, J.G. Goodwin, R. Oukaci, Journal of Catalysis 160 (1996) 125–133.

[37]. G. Jacobs, P.M. Patterson, Y. Zhang, T. Das, J.L. Li, B.H. Davis, Applied Catalysis A: General 233 (2002) 215–226.

[38]. E. Iglesia, S.L. Soled, R.A. Fiato, G.H. Via, Journal of Catalysis 143 (1993) 345–368.

[39]. M.J. Parnian, A.T. Najafabadi, Y. Mortazavi, A.A. Khodadadi, I. Nazzari, Applied Surface Science 313 (2014) 183–195

[40]. D.Y. Xu, W.Z. Li, H.M. Duan, Q.J. Ge, H.Y. Xu, Catal. Lett. 102 (2005) 229–235.

[41]. M.P. Kapoor, A.L. Lapidus, A.Y. Krylova, Stud. Surf. Sci. Catal. 75 (1993) 2741–2744.

[42]. S. Vada, A. Hoff, E. Dnanes, D. Schanke, A. Holmen, Fischer–Tropsch synthesison supported cobalt catalysts promoted by platinum and rhenium, Top. Catal.2 (1995) 155–162.

[43]. C.J. Bertole, C.A. Mims, G. Kiss, J. Catal. 221 (2004) 191–203.

[44]. D. Schanke, S. Vada, E.A. Blekkan, A.M. Hilmen, A. Hoff, A. Holmen, Study of Pt-promoted cobalt CO hydrogenation catalysts, J. Catal. 156 (1995) 85–95.

[45]. J.L. Li, X.D. Zhan, Y. Zhang, G. Jacobs, T. Das, B.H. Davis, Fischer–Tropsch synthesis: effect of water on the deactivation of Pt promoted Co/Al2O3catalysts,Appl. Catal. A 228 (2002) 203–212.

[46]. G. Jacobs, P.M. Patterson, Y. Zhang, T. Das, J.L. Li, B.H. Davis, Fischer–Tropsch synthesis: deactivation of noble metal-promoted Co/Al2O3catalysts, Appl. Catal.A 233 (2002) 215–226.

[47]. W. Ma, G. Jacobs, R. A. Keogh, D. B. Bukur, B. H. Davis, Applied Catalysis A: General 437– 438 (2012) 1– 9.

[48]. E. Iglesia, Appl. Catal. A: Gen. 161 (1997) 59–78.

[49]. B.D. Cullity, Elements of X-ray Diffraction, third ed., Addison/Wesley, Reading,MA, 1967.

[50]. G. Jacobs, M.C. Ribeiro, W. Ma, Y. Ji, S. Khalid, P.T.A. Sumodjo, B.H. Davis, Group11 (Cu, Ag, Au) promotion of 15%Co/Al2O3Fischer–Tropsch synthesis catalysts,Appl. Catal. A 361 (2009) 137–151.

[51]. N. Osakoo, R. Henkel, S. Loiha, F. Roessner, J. Wittayakun, Applied Catalysis A: General 464–465 (2013) 269–280

[52]. L.I. Ilieva, G. Munteanu, D.Ch. Andreeva, Bulgarian Chem. Commun. 30 (1998) 378.

[53]. L. Leite, V. Stonkus, L. Ilieva, L. Plyasova, T. Tabakova, D. Andreeva, E. Lukevics, Catal. Commun. 3 (2002) 341.

[54]. K. Jalama, N. Coville, D. Hildebrandt, D. Glasser, L. Jewell, J. Anderson, S. Taylor, D. Enache, G. Hutchings, Top. Catal. 44 (2007) 129.

[55]. G. Jacobs, M. C. Ribeiro, W. Ma, Y. Ji, S. Khalid, P. T.A. Sumodjo, B. H. Davis, Applied Catalysis A: General 361 (2009) 137–151

[56]. R. Riva, H. Miessner, R. Vitali, G.D. Piero, Applied Catalysis A: General 196 (2000) 111–123

[57]. H. Karaca, O.V. Safonova, S. Chambrey, P. Fongarland, P. Roussel, A. Griboval-Constant, M. Lacroix, A.Y. Khodakov, Journal of Catalysis 277 (2011) 14–26

[58]. M. Luo, H. Hamdeh, B.H. Davis, Catalysis Today 140 (2009) 127–134

[59]. Z. Pan, D.B. Bukur, Applied Catalysis A: General 404 (2011) 74– 80

[60]. V.A. de la Pen˜a O'Shea, N. Homs, J.L.G. Fierro, P. Ramı´rez de la Piscina, Catalysis Today 114 (2006) 422–427

[61]. Z. Pan, M. Parvari, D.B. Bukur, Applied Catalysis A: General 480 (2014) 79–85

[62]. B. Jongsomjit, T. Wongsalee, P. Praserthdam, Materials Chemistry and Physics 97 (2006) 343–350
[63]. L.A. Cano, M.V. Cagnoli, J.F. Bengoa, A.M. Alvarez, S. G. Marchetti, Journal of Catalysis 278 (2011) 310–320

CHAPTER 3: RESEARCH METHODOLOGY

3.1. Introduction

The central objective of this chapter is to provide information on the main steps, procedures and apparatus used in order to accomplish the goals of this project. The project was comprised of a literature review, catalyst preparation, catalyst characterization and catalyst evaluation.

3.2. Materials and chemicals used

3.2.1. Gases

All gasses used in this study were of ultra-high purity (UHP) and supplied by AFROX. The details on all gases used are outlined below.

Calibration gas mixture

This gas mixture was used to calibrate the gas chromatograph (GC) and had the following molar composition:

C_2H_4: 0.98 %

C_2H_6: 0.98 %

CO_2: 4.8 %

CH_4: 5.2 %

CO: 24.0 %

N_2: 10.4 %

H_2: Bal

Synthesis gas

The synthesis gas was used for FT runs. It contained 10 % N_2, 30 % CO with H_2 balance.

Nitrogen was used to purge and flash the system and for pressurizing the system to check for leaks before starting an FT run.

GC carrier gases

- Pure Ar was used as a carrier gas for the thermal conductivity detector

- Pure H_2 and air were used as flame gases and H_2 was also used as carrier gas for the flame ionization detector.

Gases used as reducing agents:

- 5 % H_2/Ar and 5 % CO/He were used during reduction
- 10 % H_2/Ar and 10 % CO/He were used to perform temperature programmed reduction and chemisorption.

3.2.2. Chemicals

Cobalt nitrate hexahydrate [$Co(NO_3)_2.6H_2O$] was used to load Co metal on the Al_2O_3 support. Both cobalt nitrate and the alumina support were supplied by Sigma-Aldrich.

3.3. Equipment used

Various equipment were used to achieve the objectives of this project. A drying oven was used to dry both the blank support and the impregnated support before calcination to remove moisture from the sample. The calcination oven was used to remove excess moisture in both the blank support and the impregnated support and to convert cobalt nitrate to cobalt oxide on the impregnated support.

A number of characterization procedures were employed in this project. An X-Ray diffractometer (RigakuUltima IV) was used to determine the structure of the catalyst. A Micrometritics ASAP 2460 was used to perform the Brunauer-Emmett_Teller (BET) analysis. A vega 3 XMU was used to perform scanning electron microscopy (SEM) measurement in order to determine the morphology of the catalyst. A Micrometritics ASAP 2020 was used to perform H_2-chemisorption on the catalyst. Temperature programmed reduction (TPR) was conducted using a Micromeritics Autochem II. A TESCAN Vega 3 XMU was used to perform SEM analyses.

The catalyst was tested for Fischer-Tropsch using a fixed-bed tubular reactor constructed at the university. The reactor used was 400 mm long with the internal diameter of 6 mm. Fischer-Tropsch products were analysed using a DANI Master GC.

3.4. Experimental Procedure

The various steps followed in order to accomplish the objectives of this project are detailed in this section and include catalyst synthesis, characterization and testing.

3.4.1. Catalyst synthesis

3.4.1.1. Support preparation

The support was prepared by mixing 25 g of Al_2O_3 with 20 g of distilled water and dried in air at 120 ^oC for 24 hours. The support was then calcined in air at 500 ^oC for 10 hours [1].

3.4.1.2. Catalyst preparation

The catalyst was prepared by wetness impregnation of the support using an aqueous solution of cobalt nitrate ($CoN_2O_6.6H_2O$). The impregnating solution was added to the Al_2O_3 to give a cobalt metal loading of 15 % by mass. The impregnated support was dried in air at 120 ^oC and calcined in air at 500 ^oC for 10 hours to decompose and convert the cobalt nitrate to cobalt oxide [1].

3.4.2. Catalyst characterization

3.4.2.1. X-Ray diffraction (XRD) analysis

XRD analysis was conducted on an ENRAF NONIUS FR590 powder diffractometer using Cu-Kα radiation. XRD is a quick analytical method predominantly applied to detect phases of a crystalline material and may perhaps make available evidence on unit cell sizes. The analysed sample is finely crushed, made uniform, and the average bulk structure is determined. Figure 3. 1 shows the X-ray diffractometer that was used to perform XRD analysis for this study.

Figure 3. 1: X-ray diffractometer

3.4.2.2. BET analysis

Surface area and porosity are capable of influencing the quality and usefulness of various materials. As a result, it is essential to define and manipulate them correctly. Equally, the understanding of porosity and surface area are often vital keys in understanding the structure, formation and possible uses of different natural materials. BET was employed to determine catalyst surface area and pore distribution in the catalyst. Nitrogen gas was used in all the BET surface area measurements. The analysis was done on the Micrometritics Tristar apparatus shown in Figure 3. 2.

Figure 3. 2: Micrometritics Tristar apparatus

3.4.2.3. Temperature programmed reduction (TPR) analysis

TPR analyses were performed to compare the behaviour of Co catalyst during reduction in the presence of H_2 and CO correspondingly. The first analysis was performed with a gas mixture containing 5 % H_2 in Ar and the second with 5 % CO in He. 100 mg of calcined catalyst sample were initially loaded in a U-shaped quartz tube reactor and degassed using nitrogen gas (30 ml/min) at 150 °C for 30 min and cooled to room temperature. The catalyst was subsequently subjected to a continuous flow of the reducing gas mixture (5 % H_2 in Ar or 5 % CO in He) and the reactor temperature was elevated to either 900 °C with a heating rate of 10 ^{o}C or to 350 ^{o}C (10 ^{o}C/min and maintained isothermal at 350 ^{o}C). The flow-rate of the reducing gas was kept at 30 ml/min for all the analyses and a thermal conductivity

detector (TCD) was located at the reactor outlet to quantity the amount of H_2 or CO uptake. The analysis was conducted on a Micromeritics Autochem II shown in Figure 3. 3.

Figure 3. 3: Micromeritics Autochem II

3.4.2.4. Scanning electron microscopy (SEM) analysis

SEM is a technique that produces information of a sample by irradiating sample with electrons [2]. The electrons inferat with atoms in the sample, generating information signals that can be detected and that provide data on the sample's surface topography and composition. The analysis was used to study the morphology of the catalyst. A TESCAN Vega 3 XMU was used to perform SEM analysis and is shown in Figure 3. 4.

Figure 3. 4: TESCAN Vega 3 XMU

3.4.3. Catalyst evaluation for Fischer-Tropsch reaction

The catalyst was evaluated for Fischer-Tropsch reaction in a fixed bed reactor constructed at the university. A 0.5 g sample of the catalyst was loaded in the reactor and various parameters such as the space velocity, pressure, temperature and effect of reducing gas mixture were evaluated. The catalyst was activated by reducing with either 5 % H_2 in Ar or 5 % CO in He for 17 hours to convert cobalt oxide to metallic cobalt since this is the active form for FTS. The flow rate of the reducing gas mixture was set to 30 ml/min at atmospheric pressure. The temperature was elevated from room temperature to either 350 ^oC or 300 ^oC at a rate of 10 ^oC per minute and kept there for 17 hours.

FT runs were performed using syngas as a feed containing 10 % N_2, 30 % CO and 60 % H_2. The outlet gas products were analysed using a Dani master gas chromatograph (GC) equipped with thermal conductivity detector (TCD) and flame ionisation detector (FID). Pictures showing the GC and the FT rig used in this study are shown in figure 3.5.

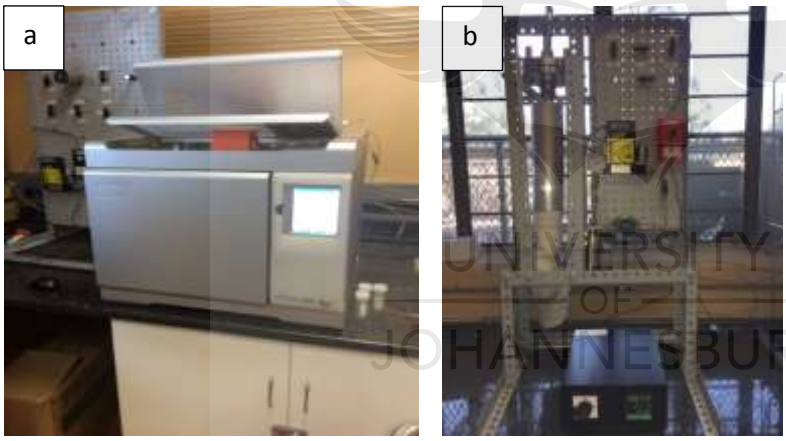

Figure 3. 5: a) Dani master GC and b) fixed bed reactor setup

N_2 (10 %) was present in the reaction feed as an internal standard used for accurate calculations of the CO conversion.

As N_2 was inert under FT conditions, its balance was written in Equation 3.1

$$\dot{n}_{T_{in}}.\%N_{2_{in}} = \dot{n}_{T_{out}}.\%N_{2_{out}} \quad \text{.....(3.1)}$$

Where $\dot{n}_{T_{in}}$ and $\dot{n}_{T_{out}}$ are the total molar flow rate in and out of the reactor and $\%N_{2in}$ and $\%N_{out}$ are the percentahe of N_2 flowing in and out respectively.

The %CO conversion was calculated as follows:

$$\%\text{CO conversion} = \frac{\dot{n}_{CO_{reacted}}}{\dot{n}_{CO_{in}}} \times 100\% = \frac{\dot{n}_{CO_{in}} - \dot{n}_{CO_{out}}}{\dot{n}_{CO_{in}}} \times 100\% \quad \text{.....(3.2)}$$

Where

$$\dot{n}_{CO_{in}} = \dot{n}_{T_{in}} \times \%CO_{in} \quad \text{..... (3.3)}$$

$$\dot{n}_{CO_{out}} = \dot{n}_{T_{out}} \times \%CO_{out} \quad \text{.....(3.4)}$$

$$\dot{n}_{T_{in}} . \%N_{2_{in}} = \dot{n}_{T_{out}} . \%N_{2_{out}} \quad \text{.....(3.5)}$$

$$\dot{n}_{T_{out}} = \dot{n}_{T_{in}} . \frac{\%N_{2_{in}}}{\%N_{2_{out}}} \quad \text{.....(3.6)}$$

After substitution of equations 3.3 to 3.6 in equation 3.2, the % CO conversion was calculated as

$$\%\text{CO conversion} = \frac{\%CO_{in} - \left(\frac{\%N_{2_{in}}}{\%N_{2_{out}}}\right) . \%CO_{out}}{\%CO_{in}} \times 100\% \quad \text{.....(3.7)}$$

The rate of CO conversion was calculated as:

$$-rCO = \dot{n}_{T_{in}} . \%CO_{in} . \frac{\%CO_{Conversion}}{100} \quad \text{.....(3.8)}$$

The rate of CH_4 production was calculated as:

$$rCH_4 = \dot{n}_{T_{out}} . \frac{\%CH_{4_{out}}}{100} \quad \text{.....(3.9)}$$

The selectivity of CH_4 was expressed as follows:

$$CH_4 \text{ selectivity} = \frac{rCH_4}{-rCO} \times 100\% \quad \text{.....(3.10)}$$

The selectivity of C_2-C_4 was calculated using the following expression

$$C_n\text{selectivity} = \frac{[(rC_nH_{n+1}+rC_nH_{n+2})\times n]}{-rCO} \times 100\% \quad \text{.....(3.11)}$$

Where n is the number of carbons (positive integer 2, 3 or 4)

The selectivity of C_{5+} was calculated as follows:

$$C_{5+}\text{selectivity} = 100\% - CH_4\text{selectivity} - \sum(C_2 + C_3 + C_4)\ \text{selectivity} \quad \text{.....(3.12)}$$

REFERENCES

[1]. K. Jalama, J. Kabuba, H. Xiong, L.L. Jewell, Catalysis Communications 17 (2012) 154–159

[2]. IHFG Seminar 2012: Nanooptics and Nanophotonics, Structural analysis of nanostructures by electron microscopy, Universitat Stuttgart, 70550 Stuttgart, Germany, July 26, 2012

CHAPTER 4: RESULTS AND DISCUSSIONS

4.1. Introduction

The results generated in this study are presented and discussed in this chapter. The data include catalyst characterization and testing results. Characterization analyses were performed on the fresh catalyst sample and on catalyst samples after reduction using 5% H_2/Ar or 5% CO/He respectively.

A number of Fischer-Tropsch reaction runs were performed using both H_2- and CO-reduced catalyst samples and various space velocities. The performance data for FT reaction, respectively over H_2- and CO-reduced catalyst samples are compared

4.2. Catalyst characterization

4.2.1. Brunauer, Emmett and Teller (BET) Analysis

BET analysis was performed on both the blank calcined ɣ-Al_2O_3 support and the fresh calcined Co/Al_2O_3 catalyst. The BET surface area, total pore volume and average pore size are presented in table 4.1 below.

Table 4. 1: Summary for BET analysis data

	Calcined blank Al_2O_3 support	Calcined 15%Co/Al_2O_3 catalyst
BET surface area [m^2/g]	123.6	110.0
Pore Volume [cm^3/g]	0.229	0.193
Pore size [nm]	56.2	62.0

The BET surface area and the total pore volume for the calcined ɣ-Al_2O_3-supported cobalt (Co/ɣ-Al_2O_3) catalyst were found to be 110m^2/g and 0.193cm^3/g respectively. These values were lower than those for the blank ɣ-Al_2O_3 support which had a surface area of 123.6 m^2/g and pore volume of 0.229cm^3/g. The decrease in surface area and pore volume after addition of cobalt metal is possibly due to some cobalt being deposited inside the pores of the ɣ-Al_2O_3 support [1]. An increase in pore size from 56.2 to 62 nm was measured upon cobalt addition to the support. This could suggest that some pores possibly collapsed during the second calcination process used to decompose the added cobalt nitrate to cobalt oxide.

4.2.2. TPR analyses

TPR analyses were performed to study the catalyst reduction behaviour in a presence of CO- or H_2-containing gas mixture. The data are presented in figure 4.1.

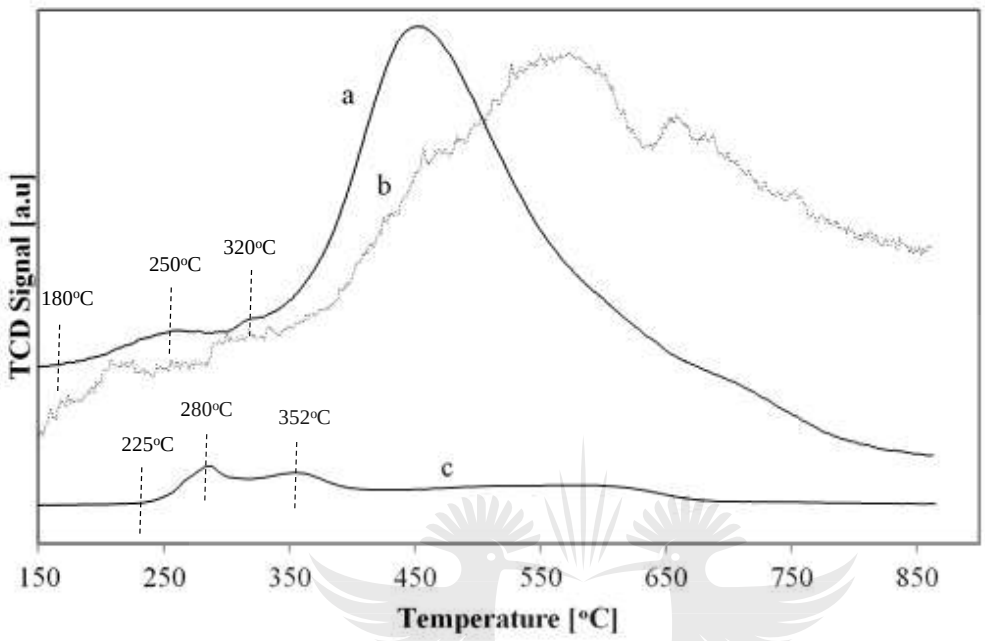

Figure 4. 1: TPR profiles for: a) blank Al_2O_3 support in presence of 10% CO/He, b) Co/Al_2O_3 catalyst in presence of 10% CO/He and c) Co/Al_2O_3 catalyst in presence of 10% H_2/Ar.

When the Co/Al_2O_3 catalyst reduction was conducted with CO/He (fig. 4.1a), the first peak started at ca. 180 ^oC and reached its maximum at ca. 250^oC. This peak was followed by a second peak with a maximum at ca. 320^oC before observing a huge peak that started at 330^oC and extended to 850^oC. To facilitate peak identification, a similar analysis was performed on a blank Al_2O_3 support and the profile is reported as fig 4.1b. Although the latter had an unstable signal, it showed a rapid increase in TCD signal that also started at ca. 330^oC and was extended to higher temperatures. This was attributed to carbon deposition on the sample. Therefore, the first two peaks observed at ca. 250 and 320^oC for the Co/Al_2O_3 catalyst in presence of 5% CO/He were respectively attributed to the two-step reduction of cobalt oxide species to CoO and Co^0 respectively following equations 4.1 to 4.3.

Step 1: $Co_3O_4 + CO \rightarrow 3CoO + CO_2$……. (4.1)

Step 2: $3CoO + 3CO \rightarrow 3Co + 3CO_2$……. (4.2)

The overall reaction is

$Co_3O_4 + 4CO \rightarrow 3Co + 4CO_2$…….…….. (4.3)

The first peak for the Co/Al_2O_3 sample in presence of 5% H_2/Ar (Fig. 4.1c) started at ca. 225 ^oC with its maximum at 280 ^oC and was attributed to the first step reduction of Co_3O_4 species to CoO. The second peak with a maximum at 352^oC was attributed to the reduction of CoO to Co^0 and was followed by an extended peak from ca. 400 to 680 ^oC attributed to the reduction of cobalt species in strong interaction with Al_2O_3 support.

The two-step reduction of cobalt oxide species in presence of H_2 can be summarized by equations 4.4 to 4.6

Step 1: $Co_3O_4 + H_2 \rightarrow 3CoO + H_2O$…….…….. (4.4)

Step 2: $3CoO + 3H_2 \rightarrow 3Co + 3H_2O$…….…….. (4.5)

And the overall reaction is written as:

$Co_3O_4 + 4H_2 \rightarrow 3Co + 3H_2O$……..... (4.6)

The data in figure 4.1 show that the two-step catalyst reduction to Co^0 using CO in He occurs at lower temperatures (ca. 30 – 32 ^oC lower) compared to reduction using H_2 in Ar. This suggests that CO improves Co/Al_2O_3 catalyst reduction.

4.3.3. XRD analyses

XRD analyses were performed on the catalyst to compare the structure of the calcined support (ɣ-Al_2O_3), the fresh ɣ-Al_2O_3-supported cobalt catalyst (Co_3O_4/ɣ-Al_2O_3) and Co/ ɣ-Al_2O_3 catalyst samples after reduction using H_2- or CO-containing gas at 300 and 350^oC respectively. The data are summarized in figure 4.2.

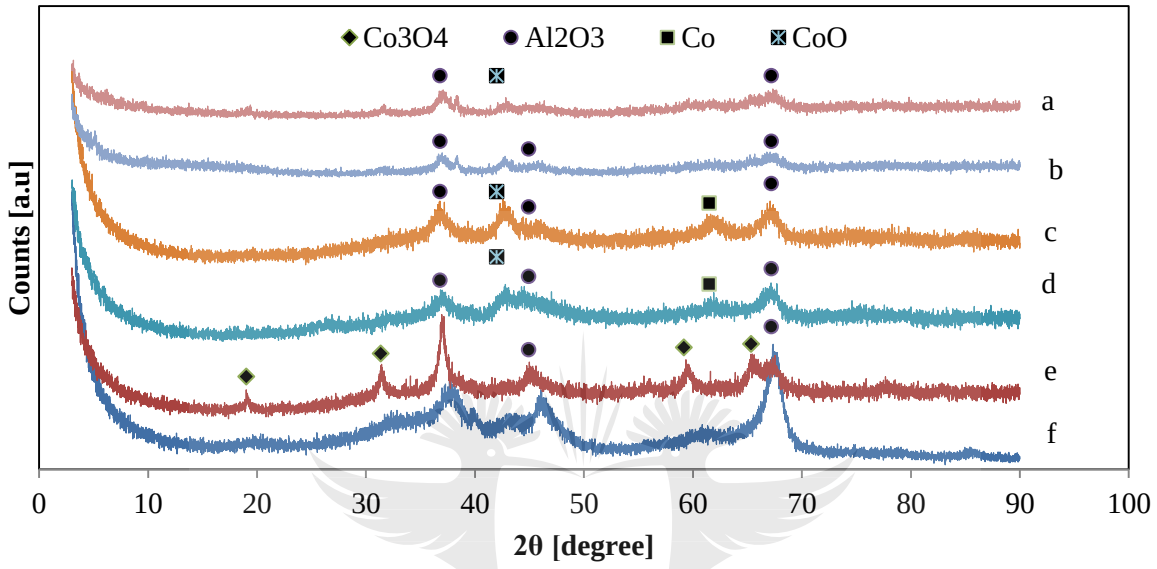

Figure 4. 2: XRD data for a) H_2-reduced catalyst at 300 ^oC; b) CO-reduced catalyst at 300 ^oC; c) H_2-reduced catalyst at 350 ^oC; d) CO-reduced catalyst at 350 ^oC; e) calcined fresh catalyst (Co_3O_4/Al_2O_3) and f) calcined blank ɣ-Al_2O_3 support

Three major diffraction peaks which were due to gamma Al_2O_3 were observed at diffraction angle 2θ equal to 39.9^o, 45.9^o and 67.7^o. Diffraction peaks corresponding to Co_3O_4 particles in the fresh calcined catalyst (fig. 4.2 e) were detected at diffraction angles 2θ equal to 19^o, 31.4^o, 59.2^o and 65.3^o. These are additional peaks which are not observed on the XRD patterns for the blank Al_2O_3 support (fig. 4.2 f). The crystallite size for Co_3O_4 as predicted using the Williamson-Hall method was found to be 50 nm.

The XRD patterns after the catalyst was activated with CO and H_2 were found to be similar. After reduction at 300^oC, both H_2- and CO-reduced (fig. 4.2 a and b) catalyst samples contained CoO as major cobalt phase. CoO and Co^0 were the major cobalt forms in the catalyst samples reduced using H_2 (fig. 4.2 c) and CO (fig. 4.2 d) at 350 ^oC.

4.1.3. SEM analyses

SEM analyses were performed to study the morphology of Co/Al_2O_3 samples after reduction using 5%H_2/Ar or 5%CO/He at 300 and 350^oC respectively. The results are summarized in figure 4.3

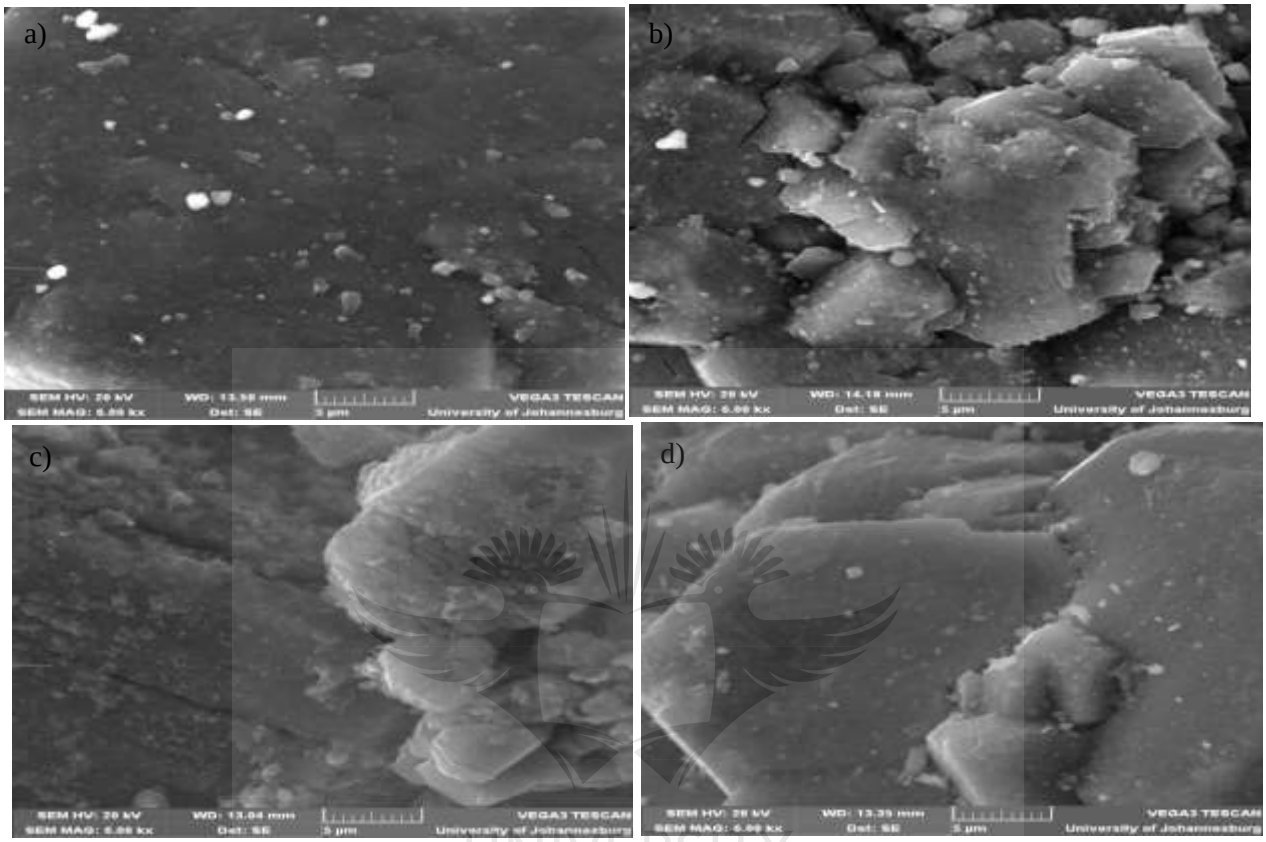

Figure 4. 3: SEM micrographs for a) CO- reduced catalyst at 300^oC, b) H_2 -reduced catalyst at 300^oC, c) CO-reduced catalyst at 350^oC and d) H_2 reduced catalyst at 350^oC.

The micrographs show some levels of coverage of CO-reduced catalyst samples (fig. 4.3 a and c) by some amorphous materials. This was not observed on H_2-reduced catalyst samples (fig. 4.3 b and d). In combination with TPR data discussed in section 4.2.2, the covering material is believed to be deposited carbon.

4.3. Fischer-Tropsch catalyst evaluation

4.3.1. Effect of space velocity on H_2-reduced Co/Al_2O_3 catalyst

The CO conversion, CH_4 selectivity and CO conversion rate results when the catalyst was reduced with 5%H_2/Ar are presented in figure 4.4 below.

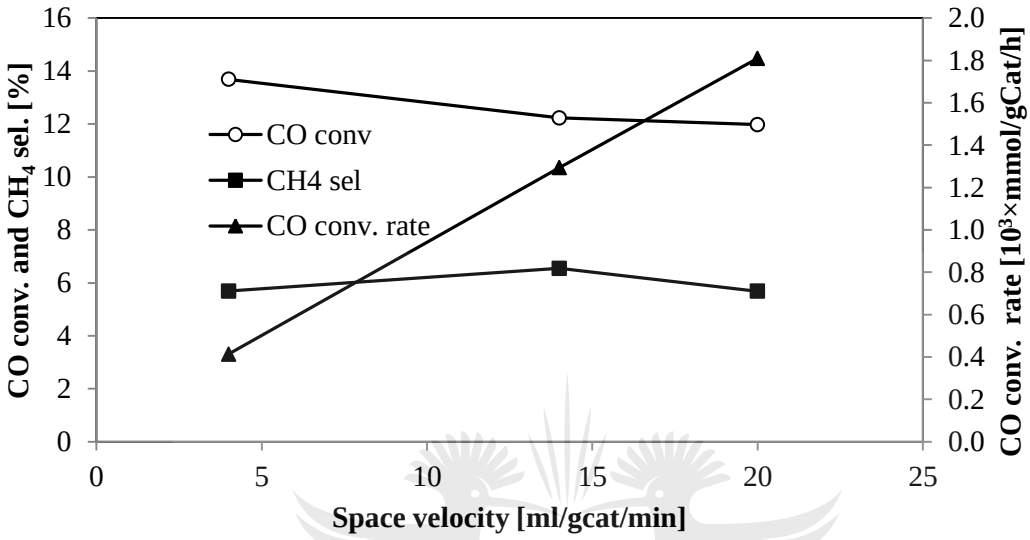

Figure 4. 4: Effect of space velocity on CO conversion, CH_4 selectivity and CO conversion rate

The CO conversion was found to possess an inversely proportional trend with respect to the space velocity. At 4 ml/gcat/min the CO conversion was ca. 13.7%. Increasing the space velocity to 14 ml/gcat/min resulted in CO conversion decreasing from 13.7% to 12.2%. Further increase of the space velocity to 20 ml/gcat/min did not significantly have an impact on the CO conversion as it only decreased to 12%. The rate of CO conversion was found to linearly increase with the space velocity. As the latter was increased from a lower value of 4 to 14 and 20 ml/gcat/min, the CO conversion rate increased from 0.414×10^3 to 1.293×10^3 and 1.810×10^3 mmol/gcat/h respectively.

Increasing the space velocity resulted in a decrease of reactants residence time in the reactor and explains the decrease in CO conversion as the space velocity was increased. The increase in CO conversion rate with an increase in space velocity can be explained by the following: i) Improved mass transfer in the catalyst. Liu *et al.*[3] also observed a similar behaviour where the specific activity of a SiC-supported cobalt catalyst increased from 0.46 to 0.55 and 0.77 g of hydrocarbons/gCat/h when the gas hourly space velocity was increased from 1900 to 2600

and 3800 h^{-1} respectively. This was explained by a higher liquid hydrocarbons removal rate from the catalyst at higher space velocities. ii) Higher reactants partial pressures at higher space velocities as the CO conversion was low. The CH_4 selectivity was not significantly affected by the space velocity as it showed a tendency to fluctuate between 5% and 6%.

Figure 4.5 shows C_{5+} selectivity as function of the space velocity

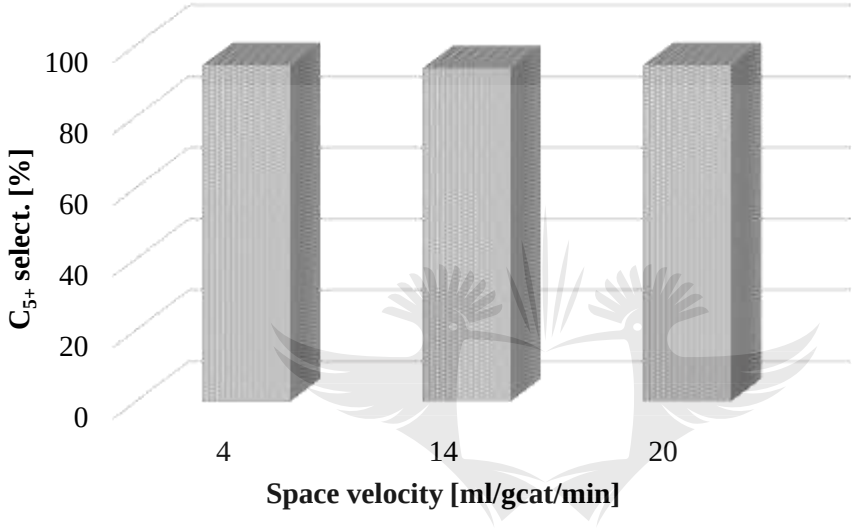

Figure 4. 5: Effect of space velocity on C_{5+} selectivity

Increasing the space velocity from 4 to 14 and 20 ml/gcat/min did not significantly affect C_{5+} product selectivity as corresponding values of ca. 94.6, 93.6 and 94.5% were respectively obtained.

Figure 4.6 shows the effect of space velocity on the olefin to paraffin (O/P) ratio.

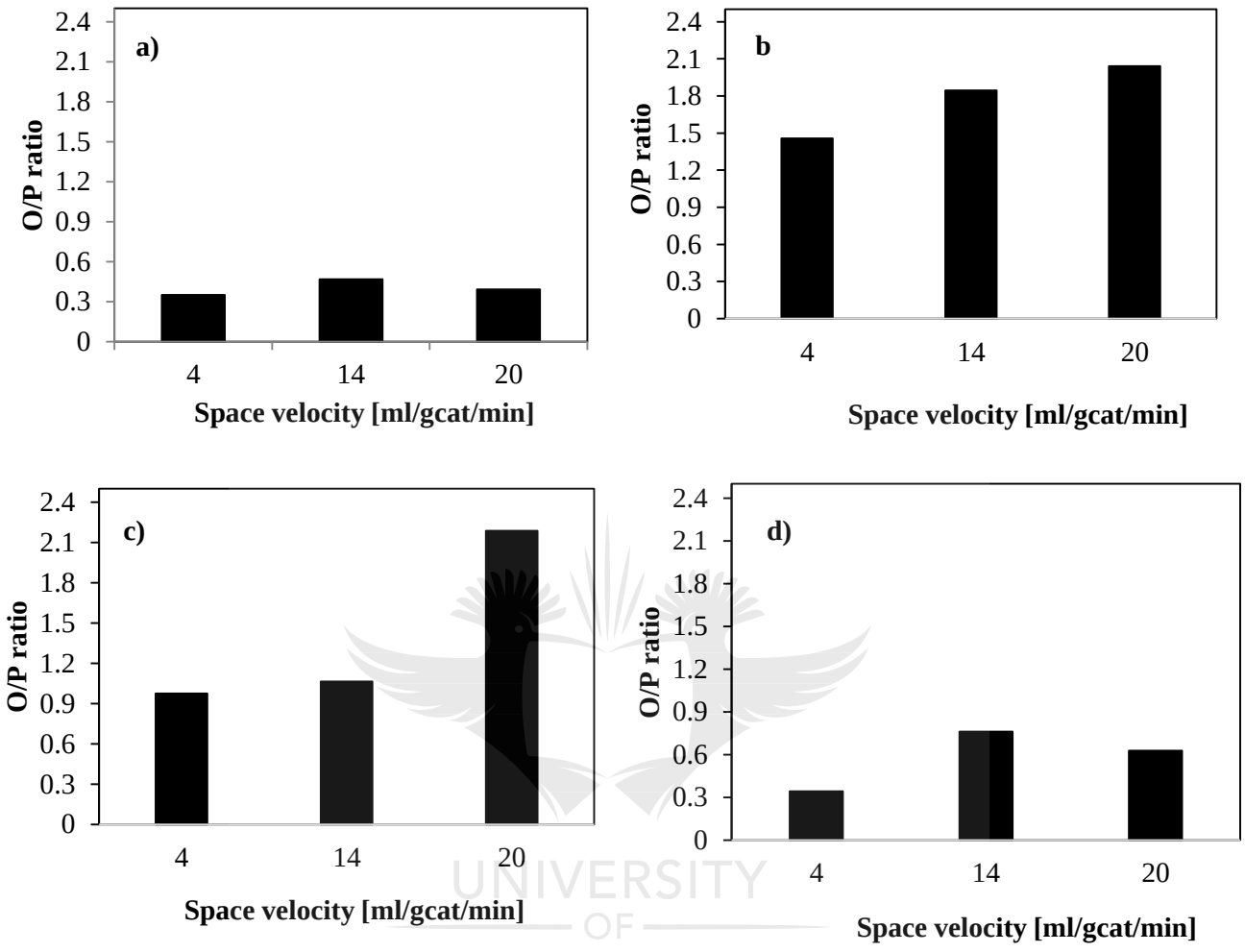

Figure 4. 6: Effect of space velocity on O/P ratio for: a) C_2; b) C_3; c) C_4 and d) C_5

The olefin to paraffin ratio for C_2 hydrocarbons did not significantly change as it remained between 0.35 and 0.47 when the space velocity was increased from 4 to 14 and 20 ml/gcat/min. On the other hand, the olefin to paraffin ratio for C_3 hydrocarbons seems to be directly proportional to the space velocity. Increasing the space velocity from 4 to 14 and 20 ml/gcat/min resulted in the olefin to paraffin ratio increasing from 1.46 to 1.84 and 2.04 respectively. A similar trend was also noticed for C_4 hydrocarbons. As the space velocity was increased from 4 to 14 and 20 ml/gcat/min, the olefin to paraffin ratio also escalated from a lower value of 0.97 to 1.06 and a higher value of 2.19. Increasing the space velocity from 4 to 14 ml/gcat/min caused the C_5 olefin to paraffin ratio to increase from 0.34 to 0.76. Further

increasing the space velocity from 14 to 20 ml/gcat/min resulted in a slight decrease in olefin to paraffin ratio from 0.76 to 0.63.

It is known that at lower space velocity the residence time increases and therefore the possibility of products formed during Fischer-Tropsch to undergo secondary reaction (i.e. hydrogenation of olefin to paraffin) increases. Thus, olefin to paraffin ratio generally increases with increasing the space velocity [4].

Figure 4.7 below shows how the space velocity influenced the chain growth probability (α) for olefin, paraffin and overall products.

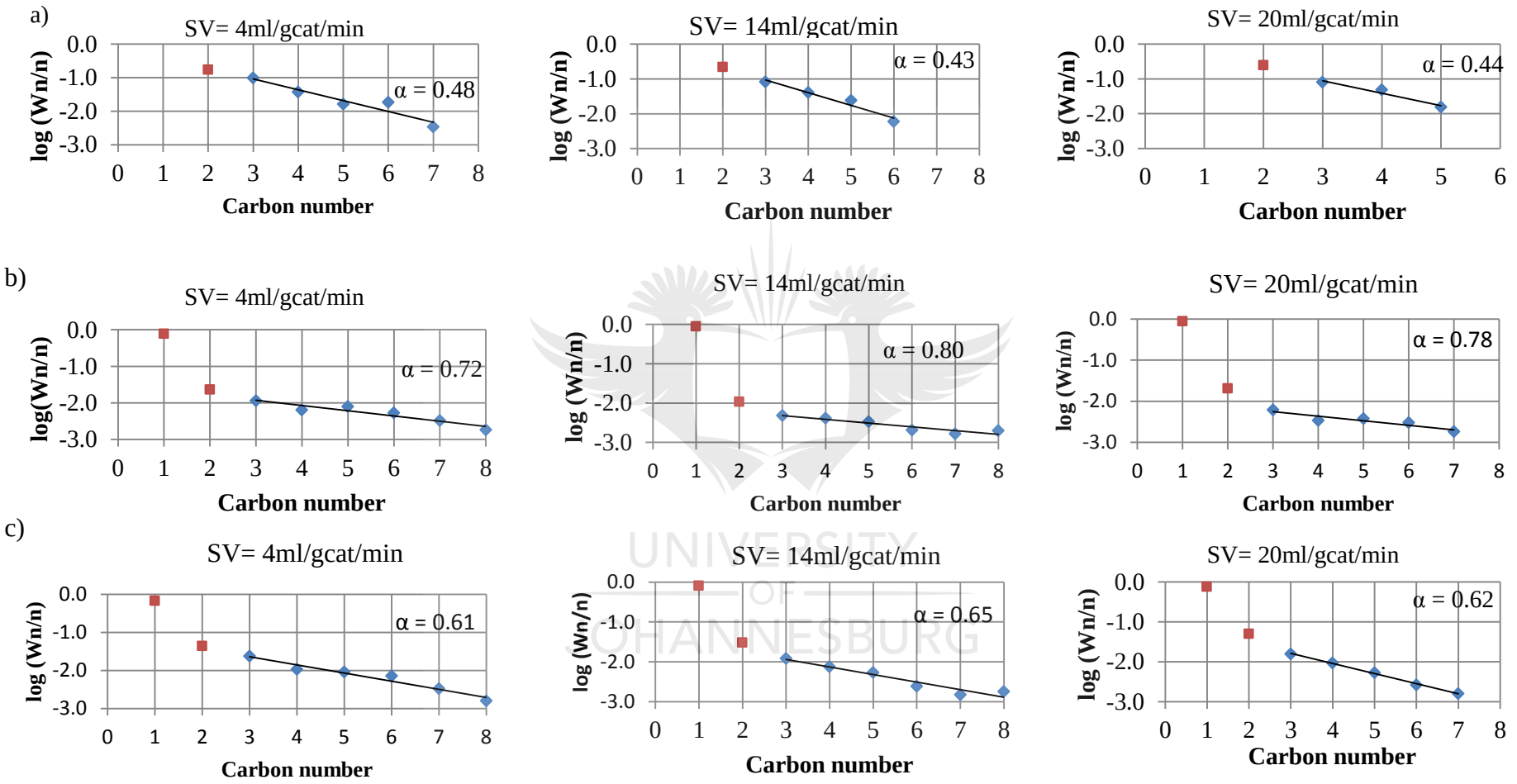

Figure 4. 7: Effect of space velocity on alpha (based on gas products) for a) olefins; b) paraffins and c) overall hydrocarbons

Within experimental error, the data suggest that the chain growth probability was not significantly influenced by the space velocity. Values for the chain growth probability of ca. 0.48, 0.43 and 0.44 for olefins; 0.72, 0.80 and 0.78 for paraffins, resulting in overall chain growth probability of 0.61, 0.65 and 0.62 were respectively obtained when the space velocity was increased from 4 to 14 and 20 ml/gcat/min.

4.3.2. Effect of space velocity on CO-reduced catalyst

Figure 4.8 below shows the CO conversion, CH_4 selectivity and CO conversion rate as function of space velocity over a CO-activated Co/Al_2O_3 catalyst.

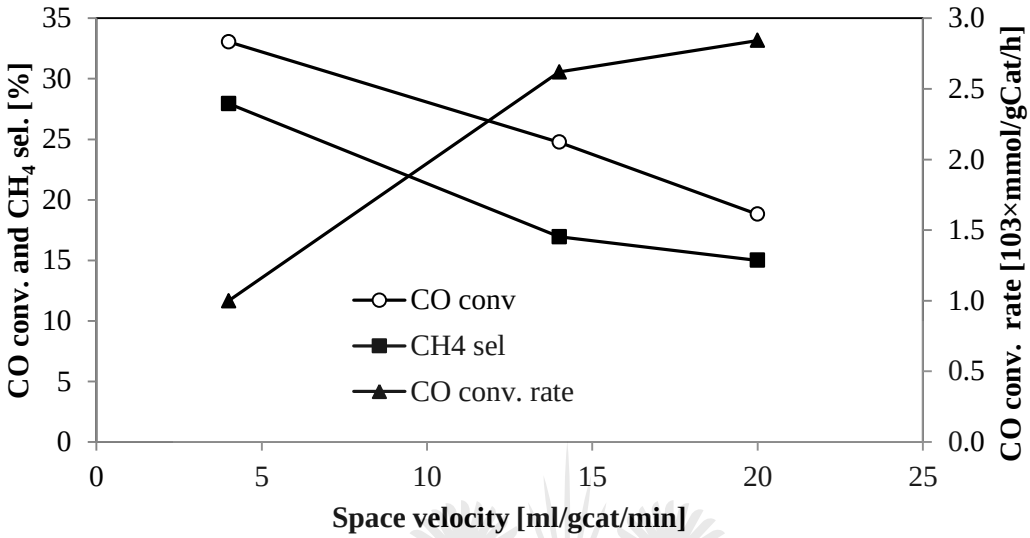

Figure 4. 8: Effect of space velocity on CO conversion, CH_4 selectivity and CO conversion rate

It was observed that CO conversion linearly decreased with increasing the space velocity. Increasing the space velocity from 4 to 14 ml/gcat/min caused the CO conversion to decline from a value of 33.1% to 24.8%. As the space velocity was further increased to 20 ml/gcat/min, the CO conversion went down to a lower value of 18.8%. As expected, the rate of CO conversion was found to increase with increasing the space velocity. As the space velocity was increased from 4 to 14 and 20 ml/gcat/min, the rate of CO conversion also increased from 0.999×10^{-3} to 2.619×10^{-3} and 2.843×10^{-3} mmolCO/g_{Cat}/h respectively. A similar trend was observed for the H_2-activated catalyst as discussed in section 4.2.1 and was explained by high rate of liquid product removal from the catalyst and high partial pressures of reactants at high space velocities.

The CH_4 selectivity was found to decrease with increasing the space velocity. When the space velocity was increased from 4 to 14 and 20 ml/gcat/min the CH_4 selectivity decrease from ca. 28 to 17 and then 15% respectively. Generally, the selectivity of CH_4 decreases with increasing CO conversion rate (lower space velocity or longer residence time). This has been reported to be a result of olefins competing with methyl groups for surface sites which in turn improves the readsorption of the olefins at lower space velocities, causing methyl

intermediates to decrease and therefore results in the decrease in CH_4 production [5]. Also, Everson *et al.* [6] investigated the effect of space velocity on product selectivity and found that at temperatures lower than 275^{o}C, as the space velocity increases, the CO conversion decreases; hence the selectivity of methane decreases and C_{5+} selectivity increases as the conversion decreases. This was explained by the hydrogenolysis of longer chain hydrocarbons at temperatures lower than 275^{o}C and low CO coverage. Secondary hydrogenolysis which may generate methane has been reported to take place on FT catalysts [3, 7].

Figure 4.9 shows the influence of space velocity on C_{5+} products

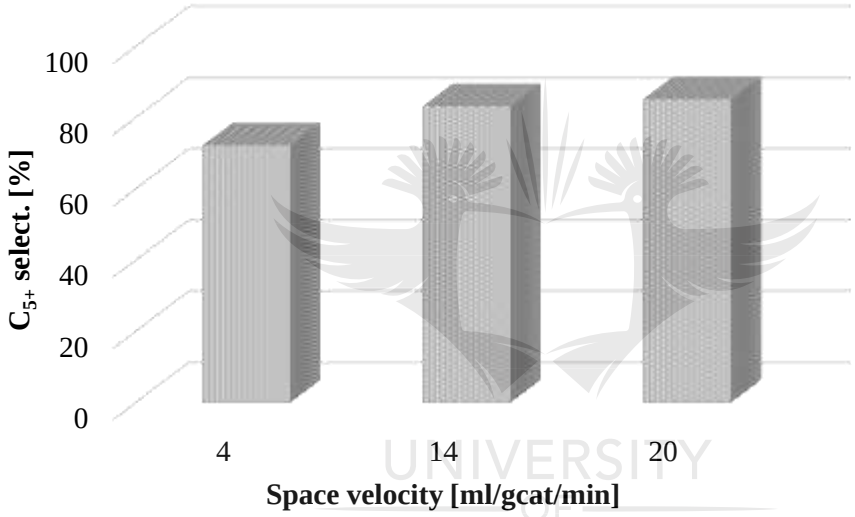

Figure 4. 9: Effect of space velocity on C_{5+} selectivity

It can be observed that the selectivity of C_{5+} products was positively influenced by increasing the space velocity. Increasing the space velocity from 4 to 14 and 20 ml/gcat/min resulted in an increase of C_{5+} products selectivity from ca. 72 to 83 and 85% respectively.

The effect of space velocity on O/P ratios is summarized in figure 4.10.

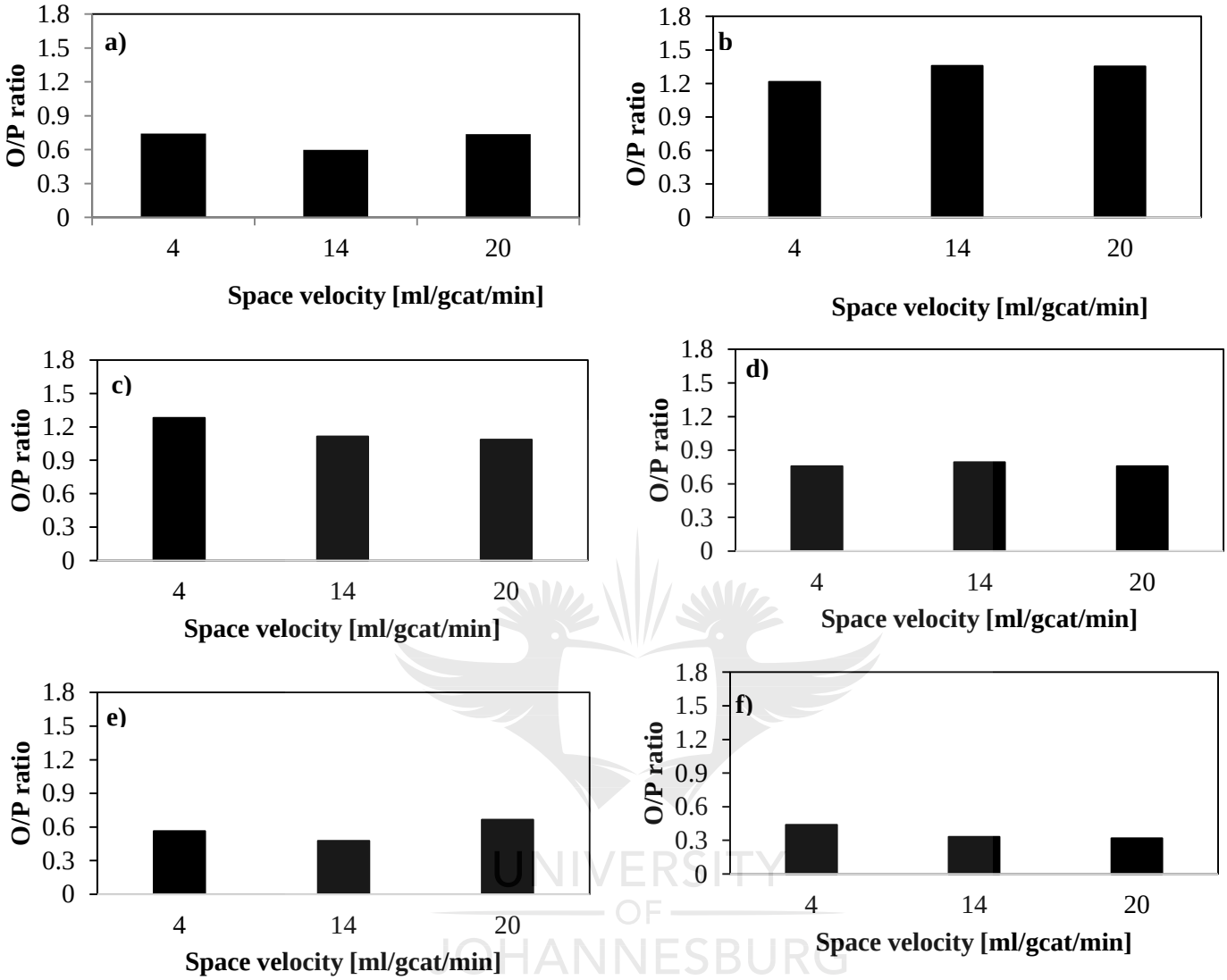

Figure 4. 10: Effect of space velocity on Olefin/paraffin ratio of a) C_2; b) C_3; c) C_4; d) C_5; e) C_6 and f) C_7

Within experimental error, the overall data suggest that the space velocity did not have a significant effect on the O/P ratio. The O/P remained around 0.59 – 0.75, 1.2 – 1.4, 1 – 1.3, 0.75 – 0.76, 0.4 – 0.7 and 0.31 – 0.45 for C_2 (Fig. 4.8a), C_3 (Fig. 4.8b), C_4 (Fig. 4.8c), C_5 (Fig. 4.8d), C_6 (Fig. 4.8e) and C_7 (Fig. 4.8f) hydrocarbons respectively when the space velocity was varied from 4 to 20 ml/gCat/min.

The effect of space velocity on the chain growth probability is summarized in figure 4.11.

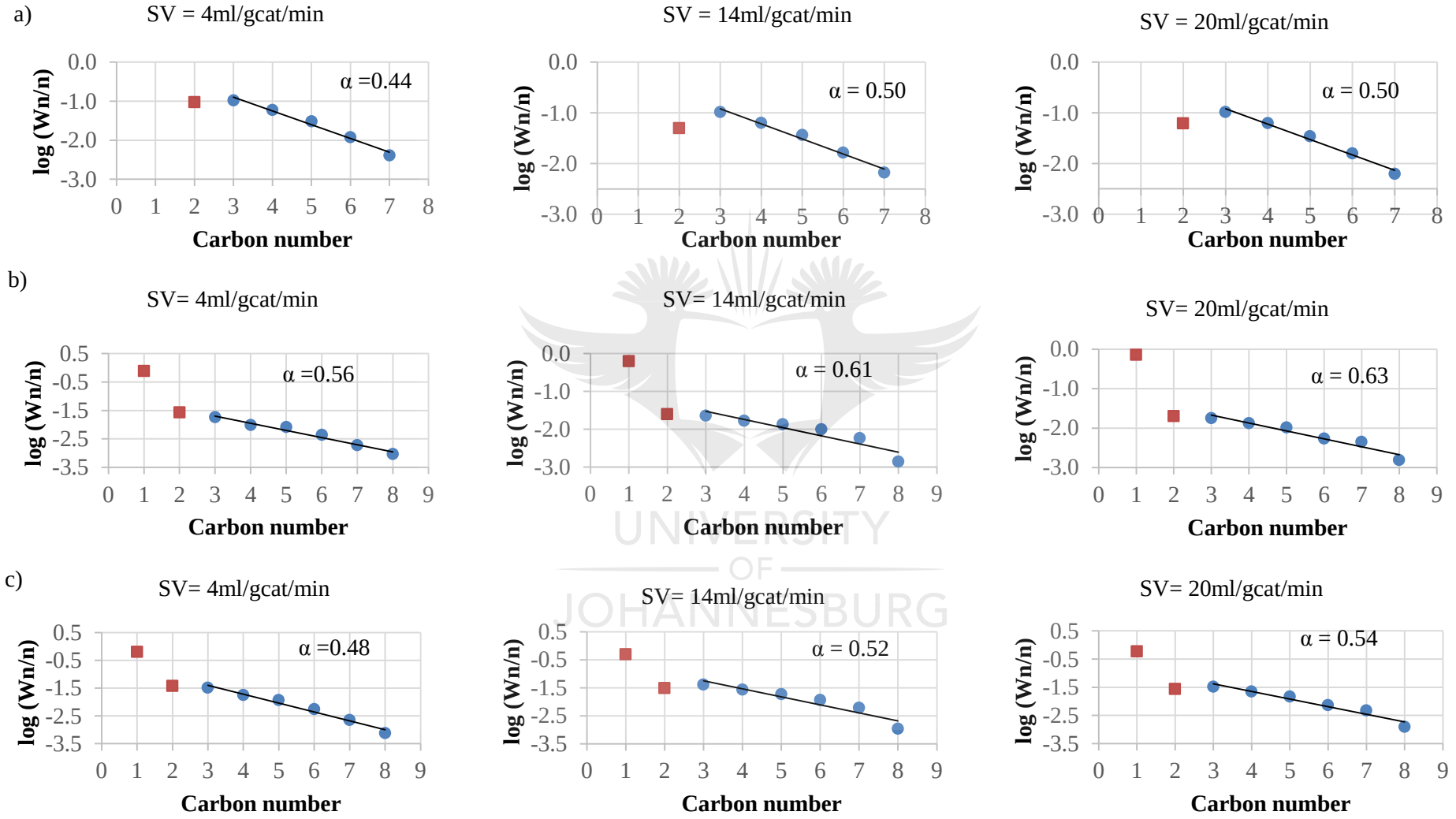

Figure 4. 11: Effect of space velocity on the chain growth: ASF plot of a) Olefin; b) Paraffin and c) Overall

It can be observed that the chain growth probability α for olefin products (fig. 4.9a) increased with increasing space velocity. Values of 0.44, 0.50 and 0.50 were obtained for space velocities of 4, 14 and 20 ml/gcat/min respectively. The alpha value for paraffins (fig. 4.9b) was also found to increase with increasing the space velocity. Increasing the space velocity from 4 to 14 and then 20 ml/gcat/min caused the chain growth probability to increase from 0.56 to 0.61 and 0.63 respectively. The overall chain growth probability (fig. 4.9c) was also found to increase with the increase in the space velocity. Values of 0.48, 0.52 and 0.54 were obtained for space velocities of 4, 14 and 20 ml/gcat/min respectively. These data are consistent with those presented in figures 4.6 and 4.8 which respectively showed a decrease in methane selectivity and an increase in C_{5+} products selectivity with an increase in space velocity.

4.3.3. Catalyst activation with CO compared to H_2

In this section, the performance of CO-activated catalyst for FT reaction is compared to that of the H_2-activated catalyst. The catalyst samples were reduced at 300 and 350^{o}C respectively. The data are summarized in table 4.2.

Table 4. 2: FT catalyst evaluation over CO- and H_2-reduced Co/Al_2O_3 catalyst

Catalyst reducing gas	Space velovity [ml/g_{Cat}/min]	Catalyst reduction temperatute [^{o}C]	CO conversion [%]	-rCO×10^3 [mol/h/gCat]	Carbon-based selectivity [%]			O/P ratio						rC_{5+} [g/gCat/h]
					CH_4	C_2 - C_4	C_{5+}	C_2	C_3	C_4	C_5	C_6	C_7	
5% H_2/Ar	20	300	11.58	1.749	3.28	0.0084	96.71	0.01	2.39	2.23	0.80	0.43	0.29	2.369
	4	350	13.69	0.414	5.69	0.0117	94.30	0.35	1.46	0.97	0.34	0.57	0.17	0.546
	14	350	12.23	1.293	6.55	0.0067	93.45	0.47	1.84	1.06	0.76	0.31	0	1.692
	20	350	11.98	1.810	5.68	0.0084	94.31	0.39	2.04	2.19	0.63	0	0	2.39
5%CO/He	20	300	14.85	2.244	8.31	0.2150	91.48	0.00	1.44	2.32	1.35	1.06	0.66	2.874
	4	350	33.05	0.999	27.94	0.1118	71.95	0.74	1.21	1.28	0.76	0.56	0.44	1.006
	14	350	24.76	2.619	16.94	0.1014	82.95	0.6	1.36	1.11	0.79	0.48	0.33	3.042
	20	350	18.81	2.843	15.00	0.0645	84.94	0.74	1.35	1.09	0.76	0.67	0.32	3.380

The data in table 4.2 show that, under similar operating conditions, CO-reduced catalyst samples exhibited higher catalyst activity and methane selectivity with higher net rate for C_{5+} formation compared to H_2-reduced catalyst samples. For example, 15% CO conversion, 8.3% CH_4 selectivity and a rate of C_{5+} production (rC_{5+}) of ca. 2.9 g/gCat/h were obtained for the catalyst sample reduced at 300^oC using 5% CO/He compared to respective values of ca. 12% CO conversion, 3.3% CH_4 selectivity and rC_{5+} of ca. 2.4 g/gCat/h] for catalyst sample reduced at the same temperature using 5% H_2/He. The high activity for the CO-reduced catalyst could be due to better catalyst reduction as suggested by TPR data discussed in section 4.2.2. The high methane selectivity measured on CO-reduced catalyst samples could be due to some possible cobalt carbide in the catalyst. Even though XRD data did not show any significant peak for cobalt carbide, the deposited carbon on the catalyst surface (as suggested by TPR and SEM data) could be the cobalt carbide precursor during FT reaction. Cobalt carbide has been reported to be more selective for CH_4 formation [8].

REFERENCES

[1]. J.W. Bae, S-M. Kim, S-H. Kang, K.V.R. Chary, Y-J. Lee, H-J. Kim, K-W. Jun, Journal of Molecular Catalysis A: Chemical 311 (2009) 7–16

[2]. K. Jalama, J. Kabuba, H. Xiong, L.L. Jewell, Catalysis Communications 17 (2012) 154–159

[3]. Liu, Y., Eduard, D., Nguyen, L.D., Begin, D., Nguyen, P., Pham-huu, C., Chemical Engineering Journal, 222 (2013) 265-273

[4]. I. Puskas, R.S. Hurlbut, Catalysis Today 84 (2003) 99–109

[5]. E. Iglesia, S.C. Reyes, R.J. Madon, Journal of Catalysis 129 (1991) 238–256.

[6]. R.C. Everson, E.T. Woodburn, A.R.M. Kirk, Journal of Catalysis 53 (1978) 186–197.

[7]. E.W. Kuipers, C. Scheper, J.H. Wilson, I.H. Vinkenburg, H. Oosterbeek, Journal of Catalysis 158 (1996) 288–300.

[8]. J. Yang, G. Jacobs, T. Jermwongratanachai, V.R.R. Pendyala, W. Ma, D. Chen, A. Holmen, B.H. Davis, Catalysis Letters 144 (2014) 123-133.

CHAPTER 5: CONCLUSIONS

The aim for this project was to investigate the effect of activating a Co/Al_2O_3 catalyst with 5% CO/He or 5% H_2/Ar on its performance for FT reaction. The catalyst was prepared by incipient wetness impregnation of the support with cobalt nitrate solution and calcined in air at 500^oC. BET, SEM, TPR and XRD analyses were used to characterize various catalyst samples. FT reactions were performed in a fixed bed reactor at 220^oC, 20 bar and space velocities of 4, 14 and 20 ml/gcat/min using CO- and H_2-reduced catalyst samples respectively. TPR data revealed that CO activates Co/Al_2O_3 catalyst at a lower temperature than H_2. Supplemented with SEM data, it was found that carbon deposits on the catalyst surface during catalyst activation with CO. XRD data for catalyst samples reduced either with CO or H_2 at the same temperature were found similar. The main form of cobalt species in catalyst samples reduced by CO or H_2 at 300 ^oC was CoO. Co^0 and CoO were the major cobalt phased for the catalyst samples respectively reduced by CO and H_2 at 350 ^oC.

Under similar catalytic testing conditions, CO-activated catalyst samples displayed higher catalytic activity for FT reaction with higher rate of C_{5+} hydrocarbons formation than H_2-activated samples. The high methane selectivity measured on CO-reduced catalyst samples is believed to be due to some possible cobalt carbide in the catalyst. It is believed that the deposited carbon is the precursor for cobalt carbide formation during FT conditions.

APPENDIX

Appendix A: Example of GC chromatogram

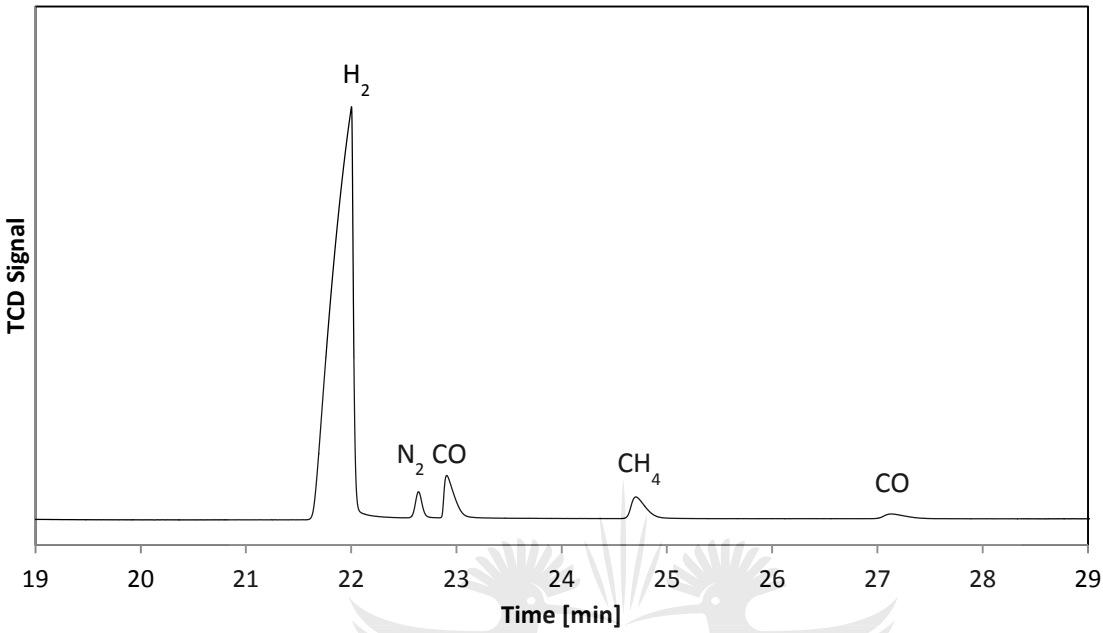

Figure A1: TCD chromatogram

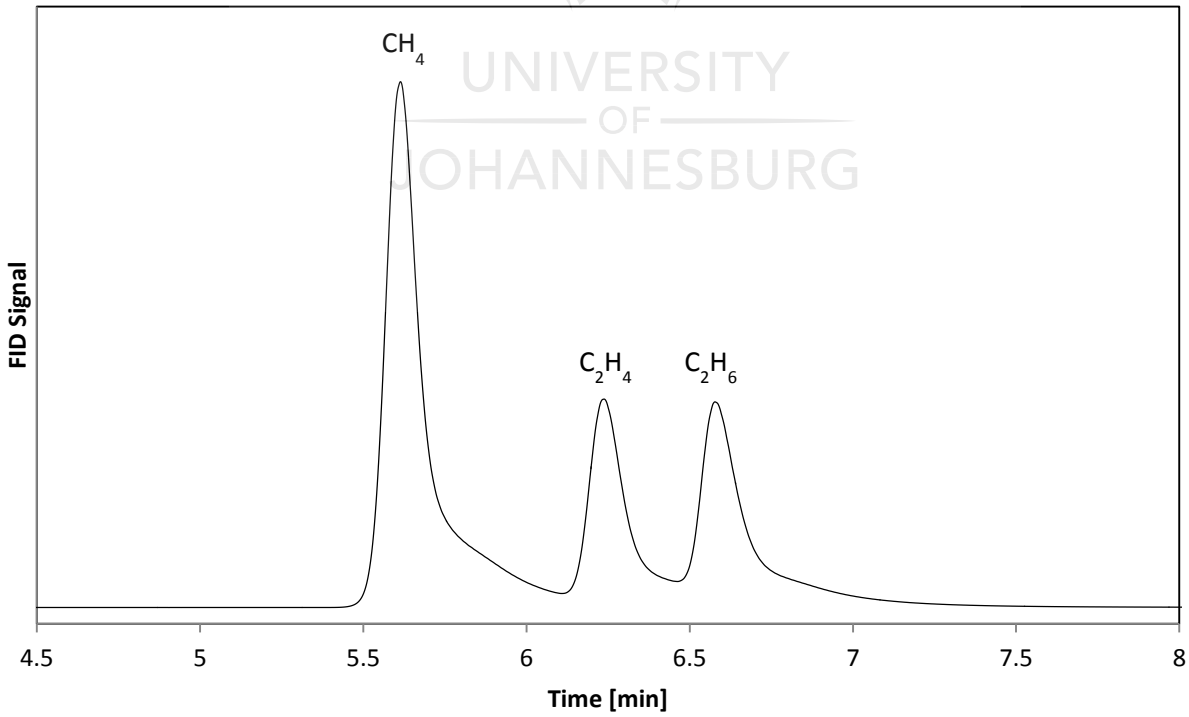

Figure A2: FID chromatogram